TOWARDS MAKING A BETTER IN VITRO MODEL OF HUMAN UPPER GASTROINTESTINAL TRACT EPITHELIA

A Dissertation

Presented to the Faculty of the Graduate School

of Cornell University

In Partial Fulfillment of the Requirements for the Degree of

Doctor of Philosophy

by

Jiajie Yu

January 2013

TOWARDS MAKING A BETTER IN VITRO MODEL OF HUMAN UPPER GASTROINTESTINAL TRACT EPITHELIA

Jiajie Yu, Ph. D.

Cornell University 2013

In vitro models of human small intestine play a critical role in predicting oral drug absorption efficiency as well as understanding intestinal epithelia functionality. Conventional 2D in vitro models fail to represent small intestinal villi which are important 3D features for the small intestinal microenvironment. Without these features, in vitro models of the small intestine lack physiological relevance. By using microfabrication techniques, we created a plastic template with accurate dimensions and densities of human small intestinal villi. Based on this template, we fabricated collagen villous scaffolds utilizing a sacrificial hydrogel technique. By integrating collagen villous scaffolds into a custom designed insert kit, we developed the first 3D in vitro model of the human small intestine. Epithelial cells cultured on this 3D model presented unique cell differentiation morphology similar to human small intestine epithelia. Drug permeability tests conducted on this 3D model provided more accurate results for drugs absorbed through the paracellular pathway when compared to conventional 2D models. In addition, alternative biomaterials were tested for their potential in making 3D villous scaffolds. This work suggests that the 3D in vitro model of the human small intestine is an effective tool for predicting drug permeability as well as investigating the small intestinal microenvironment.

BIOGRAPHICAL SKETCH

Jiajie Yu was born in Beijing City, China. He is the only child of a working class family. At the age of 4, Jiajie started playing the violin. He was admitted to Beijing Juvenile Golden Sail Symphony Orchestra and then Beijing Golden Sail Symphony Orchestra for playing the viola, where he rehearsed and toured with the orchestra regularly. At the age of 15, Jiajie started playing guitar which became the biggest hobby in his spare time. After graduating from Beijing 101 middle school, Jiajie was admitted to Zhejiang University studying Bioengineering as well as Zhejiang University Wenqin Symphony Orchestra for playing the viola. When maintaining high academic standards, Jiajie also formed his college rock band which was popular around the campus. In his junior year, Jiajie joined Dr. Zhinan Xu's lab at Zhejiang University working as an undergraduate research assistant. Then he was selected into the student delegation attending a summer exchange program between Cornell University and Zhejiang University. During this time, Jiajie met his future advisor Dr. John March and discussed his graduate study plan with him. Luckily enough, Jiajie was admitted to Cornell University to study Biological Engineering and became the first graduate student of Dr. John March. During his graduate training, Jiajie became capable of various engineering problems including fixing his car and overhauling an old boat. When Jiajie was not working in the lab, he was enjoying Ithaca by doing wakeboard at Cayuga Lake or playing in the blues jam at a local bar, the Nines.

ACKNOWLEDGMENTS

I consider conquering this Ph.D. degree at Cornell to be the toughest goal I have ever achieved since I was born. I would like to give my sincerest acknowledgments to the following people for helping me become the ultimate nerd. First, I would like to thank my advisor Dr. John March for his great patience and encouragement. I feel extremely lucky that I had the chance to work under such a nice advisor and we truly became good friends. I would also like to thank my committee members, Dr. Dan Luo and Dr. Antje Baeumner for their support throughout my Ph.D. training. I would like thank my former collaborators Dr. Jong Hwan Sung, Songming Peng and Dr. Cait Costello. It is my honor to have had the chance to work with those great researchers. I would also like to thank my oldest labmate Dr. Faping Duan for his great support over five years. I would like to thank my friends Chris Aurand, Kitiya Vongkamjan, Matthew Russell and Tom Derrien for sharing lots of good times. I would also like to thank my guitars and the great rock and roll for keeping me relaxed. Finally, I would like to thank my family members, especially my parents, for the long-time support.

The time I spend at Cornell has made me become a much more capable man. I will always value this precious experience in my life.

TABLE OF CONTENTS

PREFACE

This dissertation was written based on the “papers option”, which means that the dissertation is composed of three research papers (which were either submitted or published during my Ph.D. study), one additional chapter and the final conclusion. The first chapter is a review paper about current in vitro small intestinal models with focuses on cellular physiology, extracellular topography and applications. The second chapter describes a novel method for fabricating 3D human small intestine villous scaffolds by combining laser fabrication and sacrificial molding technique. The third chapter describes how we developed the first 3D human small intestine in vitro model, which not only presented unique cellular differentiation morphology but also obtained a better permeability correlation to human intestines for paracellular pathway transported drugs. The fourth chapter introduces an alternative material which was tested for its potential for making villous scaffolds. In the final conclusion, I gave my personal insights and ideas for future directions of this project. We started this project without much precedent in the area of making synthetic villi. There are still many challenging problems that need to be solved and I hope this dissertation is a helpful resource for future research.

Jiajie Yu

Ithaca, New York

December 2012

CHAPTER ONE:

SYNTHETIC SMALL INTESTINES FOR STUDYING INTESTINAL FUNCTION AND HOST-MICROBIAL INTERACTIONS

Yu J [a], Costello CM [a], March JC [*a] (2012) Synthetic Small Intestines for Studying Intestinal Function and Host-Microbial Interactions. Submitted to Medical & Biological Engineering & Computing

[a] Biological and Environmental Engineering, Cornell University, USA.

ABSTRACT

In vitro small intestinal models not only play a critical role for understanding small intestine functionality, predicting oral drug absorption efficiency and investigating cell differentiation mechanisms but are also becoming more important for illustrating complicated interactions between intestinal epithelial cells and commensal bacteria. In this review, in vitro small intestinal models are discussed with respect to cellular physiology and excellular topography. The roles of in vitro small intestinal models in investigating GI host-microbial interactions are discussed.

INTRODUCTION

Creating in vitro artificial small intestines that realistically mimic in vivo systems is one of the most exciting and promising areas of biotechnology [1, 5, 70], with potential to aid in the study of many under-researched gut disorders including Crohn's disease [16], irritable bowel syndrome [46], short-bowel syndrome [48] and gastroenteritis [47]. Typically intestinal function and disease processes are assessed in vivo using live animal models [57], however multiple studies have shown that these models often do not correlate well with human systems [50], and are expensive and time consuming as well. Additionally, animal models do not allow for real-time visual documentation of cellular growth and survival, and they present limitations for control and manipulation of specific intestinal processes. In contrast, synthetic in vitro intestinal models can potentially enable improved studies of intestinal function in an ethically and well controlled manner, in particular for studies of cellular growth and proliferation [10], drug absorption [77] and host-microbial interactions [8].

The challenge is to construct a synthetic in vitro model that is topographically, mechanically and chemically similar to native tissues. The small intestine is a dynamic organ, displaying a structurally complex array of surface features that are home to a confluent layer of many different cell types that allow it to perform its primary functions of digestion and absorption (Figure 1.1). The circular folds of the intestinal mucosa, with fingerlike protrusions of up to 1.5 mm in length (intestinal villi) extending out into the lumen, form an intricate 3D environment. Each villus has lamina propria (loose connective tissue) as a core where the blood capillary network, lymphatic vessel, nerve fibers and various cells of the immune system are located [6, 22]. Small intestinal stem cells which reside in crypts of Lieberkühn differentiate into four different small intestine epithelial cell types including enterocyte cells (absorptive cells), goblet cells, enteroendocrine cells and paneth cells. While forming tight junctions as a barrier between the lumen and lamina propria, the small intestinal epithelia undergo vigorous cell proliferation and differentiation processes where cells on the villi are renewed every 4-5 days [72].The small intestine is also heavily populated with microorganisms [39], which increase in concentration along the length of the intestine from 10^4 cells/g in the duodenum to 10^{12} cells/g in the colon [35]. In addition to the complex topographical and cellular environment, the human intestine exhibits mechanically active peristalitic motions and fluid flow (mediated by the intestine's own nervous system and smooth musculature), which strongly affect the microenviroment and surface morphology.

There exists a wide variety of models designed to study intestinal function, from small scale systems including simple porous cellular supports and microfluidic devices to large bioreactors. Each model has its own strengths and weaknesses in terms of complexity, and therapeutic relevance. This review aims to introduce the reader to the principal considerations for constructing a realistic in vitro intestinal model: including the different cell types, biomaterials and mechanical devices available. In addition, this review will give an overview of the current status of artificial small intestinal engineering for studying both intestinal function and host-microbial interactions.

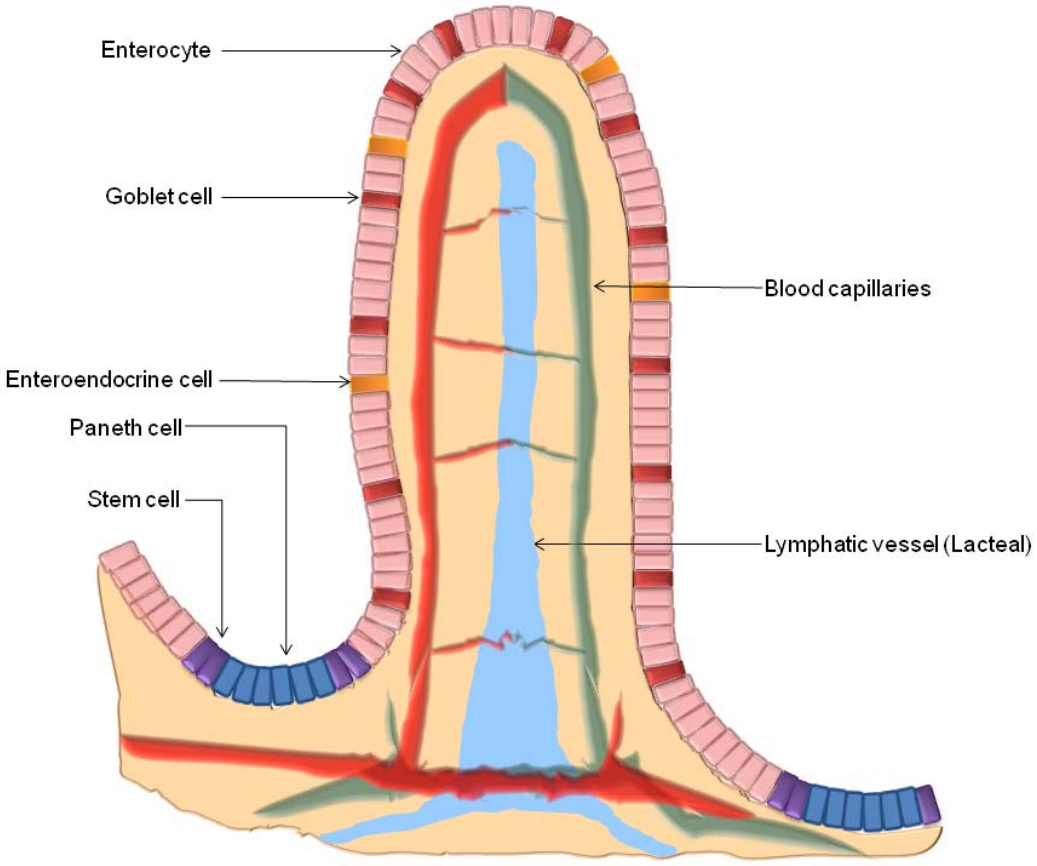

Figure 1.1 Cross section of a small intestinal villus

SMALL INTESTINAL EPITHELIUM: CELLULAR CONSIDERATIONS

Perhaps the one of the most important considerations for the construction of an in vitro intestinal model is the cellular composition. At its simplest, a single cell type can be used for studying cellular responses to surface topography and/or environmental cues; however, models consisting of multiple phenotypes are desirable for the dynamic study of cellular interactions. Cell culture techniques are continually advancing, allowing for the co-culture of a variety of cell types on suitable surface supports.

Enterocytic cell lines

Enterocytes are the most abundant cell type among the intestinal epithelium, with each cell exhibiting a brush border membrane of up to 3000 microvilli upon differentiation [15]. The brush border also produces digestive enzymes such as peptidases and disaccharidases [65], as well as various nutrient transporters including sugar, amino acids, vitamins and minerals [18]. As the main cellular constituent of the small intestine, enterocytic cell lines form the basis of the simplest in vitro intestinal models. The most common and extensively studied is the human epithelial colorectal adenocarcinoma cell line (Caco-2) [26]. When forming a monolayer, Caco-2 cells can spontaneously differentiate into columnar and polarized cells that possess many similar characteristics of small intestinal enterocytes, including tight junction and microvilli formation as well as intestinal transporter and digestive enzyme expression [26, 53]. Caco-2-based intestinal models are thereby widely used for investigating functionalities of different intestinal transporters, determining nutrient bioavailability and predicting oral drug absorption efficiency [3, 25, 45]. Additionally, Caco-2 cells

can be converted into M cells in vitro by culturing lymphoid cells at their basolateral side. When cultured in this way, Caco-2 cells are capable of transporting antigens in a manner similar to M cells [31].

However, since Caco-2 cells are derived from the colon, rather than the small intestine, they have significantly different gene transcriptional profiles compared to native host upper intestinal cells, suggesting there may be key differences in enzymes and transporter availability between the two [69]. It has also been speculated that Caco-2 monolayers exhibit diminished porosity, as studies have shown they have increased trans epithelial electric resistance (TEER) compared to human small intestinal epithelium. Poor porosity would also explain the poor paracellular drug permeability correlations between in vivo and in vitro models using Caco-2 cells [3, 55]. Cell lines such as the Madin-Darby canine kidney (MDCK) and the rat intestinal 2/4/A1 have been considered as an alternative for in vitro intestinal models due to their low monolayer TEER values [29, 71]. However, a recent study found that Caco-2 monolayers and MDCK monolayers have similar pore sizes and only 2/4/A1 monolayers present a porosity that is similar to human intestinal epithelium [41].

Goblet cell lines

Goblet cells secrete various glycoproteins called mucins, which are the main component of the intestinal mucus layer. While providing defense of intestinal epithelium against excessive mechanical stress and toxic chemical agents, the mesh-like network of mucin also prevents intestinal microbial invasion without impeding

nutrient transport [34]. Besides mucins, goblet cells also secrete intestinal trefoil factor peptides and resistin-like molecule β, which are both involved in mucin stabilization and mucin secretion regulation [17]. Due to the critical function of a mucin layer in small intestinal immunity, more complex in vitro models can benefit from co-culture with goblet cell lines (such as HT29-MTX) in addition to enterocytes [74]. Originally isolated as an undifferentiated human colon carcinoma cell line, HT-29 was initially used to mimic intestinal enterocytes when cultured under selective conditions [52]. However, later studies found that HT29 could differentiate into mucus producing, goblet-type cells after stimulation with the anticancer drug methotrexate (MTX). This MTX adopted cell line (HT29-MTX) retained the differentiated phenotype even in MTX-free medium [38]. The TEER values of co-cultured monolayers of HT29-MTX and Caco-2 have been found to be lower than purely Caco-2 cultures, which also provided paracellular drug permeability that is more similar to the case in vivo, although the improvement was limited [73].

Besides drug permeability determination, Caco-2 HT29-MTX co-culture models have also been used for studying iron bioavailability, since mucus layers are involved in iron absorption [45]. More recently, lymphoid cells were added to the basolateral side of a Caco-2/HT29-MTX co-culture model to stimulate M cell conversion. This tri co-culture model was used to investigate nanoparticles effects on iron absorption [44]. Moreover, HT29-MTX cultures provided in vitro evidence that mucus production is linked to bacterial signaling, and mucus layers play an important role in bacterial adhesion as well as small intestinal epithelium inflammation [36, 49, 66].

Enteroendocrine cell lines

Enteroendocrine cells represent less than 1% of the entire intestinal epithelial population, although there are up to 15 different subtypes [68, 72]. Enteroendocrine cells are highly sensitive to luminal contents, and as such more than 30 hormones are released in response to specific stimuli [2, 11], which enable regulation over small intestinal motility, blood flow and secretion [11, 28]. The availability of a human enteroendocrine cell is rare for use in in vitro models, therefore immunoreactive alternatives including murine intestinal tumor cell lines such as STC-1 and GLUTag are often used [19, 60]. Both cell types have been exploited to study mechanisms of hormone secretion, such as cholecystokinin and glucagon-like peptide-1 in vitro [23, 30, 64]. STC-1 has also been found to produce 'bitter taste' receptors, which provided evidence to suggest that the small intestinal epithelia are involved in overall taste-sensing mechanisms [75].

Crypt cell lines

In vitro crypt cell lines have been established and extensively used to understanding small intestinal epithelium differentiation. For example, rat small intestinal epithelial cells have been isolated and established for subculture in vitro [56]. Among these rat small intestinal epithelial cell lines, IEC-6 has been the most frequently used cell type to investigate differentiation signals. Under normal culture conditions, IEC-6 retains the characteristics of undifferentiated small intestinal crypt cells [56]. When cultured on the extracellular matrix Matrigel, IEC-6 cells become more differentiated and exhibit several enterocyte characteristics such as being polarized with microvilli on

their apical side and expressing digestive enzymes [12]. Recently, a clone of IEC-6 which over expresses transcription factors Cdx2 and HNF-4α not only obtained differentiated enterocyte characteristics but also expressed mucus related gene mucin 3 when cocultured with intestinal mesenchymal cells in vitro [43]. Moreover, a clone of IEC-6 expressing the insulin promoting factor PDX-1 had pancreatic β -cell like characteristics including secreting insulin, which when transplanted in adult diabetic rats showed potential as a diabetes therapy [76].

In vitro crypt cell lines were also established from human small intestine. For example, the HIEC cell line, which retains undifferentiated crypt cell characteristics was developed from human small intestine [51]. Highly similar to IEC-6, HIEC was used to investigate the function of transcription factors Cdx2, HNF-1α and GATA-4 in enterocyte differentiation. Combining expression of these three transcription factors made HIEC differentiate into an enterocyte morphology with digestive enzyme gene expression [7]. Interestingly, Sato et al. [62] have successfully demonstrated that a single mouse stem cell could not only differentiate into the four different small intestinal epithelial cell types but also could form crypt-villus like structures in vitro. Similarly, Spence et al. [67] have differentiated human pluripotent stem cells into crypt-villus-like 3D organoids that appear to maintain the complete function of small intestinal epithelium. These novel stem cell culture methods not only provide new insight into small intestinal development but also greatly improve in vitro model capabilities.

SMALL INTESTINAL TOPOGRAPHY: CELLULAR SUPPORTS AND BIOMATERIAL CONSIDERATIONS

Cultures of intestinal cells usually make use of a porous scaffold to provide a surface for cell seeding and proliferation, as well as the mechanical/physical support (stiffness) needed for cell growth. A common method is to seed on the classic transwell insert, which has a micro-porous plastic membrane as the growth surface [26, 27]. These transwells are produced via a track-etching process and have well controlled pores that range from 0.4µm to 8µm in diameter, which allow media and molecules to pass through freely while blocking epithelial cell migration [21]. The apical side of a transwell is considered to be the luminal side whereas the basolateral side of transwell is termed the submucosal side (Figure 1.2A). Compared to a normal cell culture well plate, which has a non-porous growth surface, the porous membranes make co-culturing of multiple cell layers possible as the cells on the bottom (basolateral) layers will not be deprived of nutrients and oxygen.

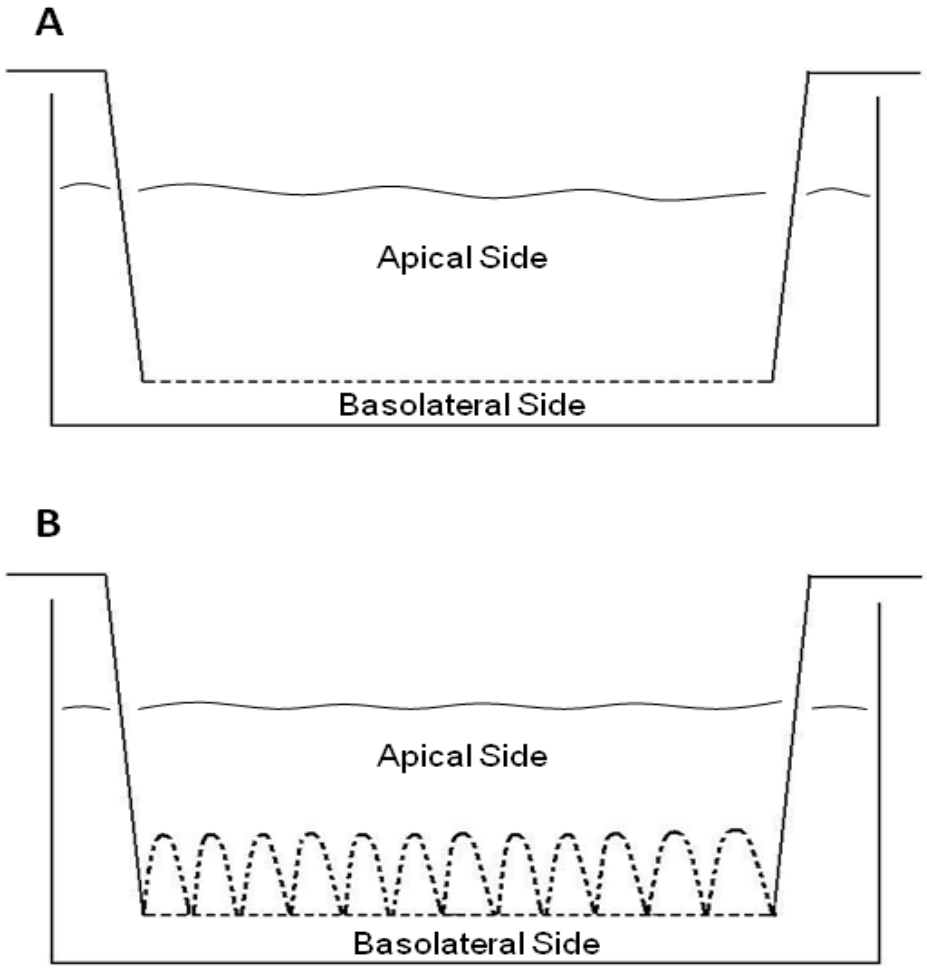

Figure 1.2 Schematic illustration of in vitro small intestinal models. (A) Transwell insert (B) Porous 3D scaffold

Although flat porous inserts have enhanced intestinal cell culture capabilities, cells seeded onto flat supports exhibit markedly different phenotypes to cells in vivo [63], as cell physiology, morphology and behavior is often determined by the physical and chemical state of the extracellular environment in which they grow. Cells in a 3D

villous environment will experience radically different gradients of nutrients and oxygen than cells grown on a flat surface [24], which will affect cell behavior and differentiation, as well as spatial differences which will affect individual cell-cell and cell-matrix contacts and communication [14, 42]. Porous 3D scaffolds are therefore becoming more commonplace in intestinal engineering (Figure 1.2B). For example, using microfabrcation techniques and hydrogel biomaterials, Sung et al. [70] constructed artificial 3D villi composed of hydrogel scaffolds in the same shape, size and distribution as human intestinal villi. A 3D human small intestinal in vitro model has been developed by Yu et al. [77] based on this technique, which presented unique differentiation morphology of Caco-2 monolayers along the crypt-villus axis. Paracellular drug permeability determined from this 3D in vitro model was more highly correlated with that of perfused human intestine than a 2D (flat) model. Further, TEER measurements in the 3D model were closer to rat TEER values than were the same measurements made in the 2D case [77]. This suggests that missing villous geometry instead of the smaller porosity of Caco-2 monolayers is the main reason for the poor paracellular drug permeability correlations in the conventional in vitro model. Along the same lines, Pusch et al developed [54] a dynamic 3D in vitro co-culture model by culturing Caco-2 cells with primary human microvascular endothelial cells (hMECs) on decellularized pig small intestine segments. While higher dipeptidase enzymatic activity and improved paracellular drug permeability was found in this 3D tissue model no TEER values were measured in this system.

HOST-MICROBIAL INTERACTIONS: CURRENT STATE OF PLAY

Perhaps one of the greatest challenges facing intestinal engineering is the ability to construct an accurate in vitro model that has the ability to support both host mammalian cells and microbial organisms. Short term co-culture models have provided evidence that host cell growth, morphology, differentiation and secretion systems are affected by the presence of microbes in the same environment. Many in vitro studies have focused on bacterial adhesion to intestinal cell lines using simple transwell plate co-culturing techniques. For example, commensal bacteria such as Lactobacillus have been found to produce proteinaceous adhesion factors, which enable them to bind the mucus secreted by goblet cells such as HT29-MTX [8]. Brovko et al. [9] applied a simple yet direct method to quantitatively assess adherence and growth of pathogenic and non-pathogenic E. coli in the presence of mammalian cells seeded on microwell plates by using bacterial strains containing bioluminescent T7 plasmids. They found that bacteria in direct contact with HeLa cells experienced greater growth than control strains incubated with FBS. In addition, bacterial translocation across Caco-2 monolayers has been found to be related to tight junction integrity, with greater levels of translocation from a short term culture with lower TEER levels [13]. Short-term co-culture models on flat inserts have also been used to elucidate the beneficial effects of probiotic microorganisms against harmful pathogens, as they stimulate the native epithelial cells to improve barrier function [37, 59].

However, these simple co-culture models provide limited data as typically long-term prolonged co-culture of intestinal cells with bacteria is poorly sustained due to differing growth rates. Microbes, as a rule, tend to multiply at a greater rate than host cells which can lead to bacterial overgrowth and accumulation of harmful metabolites [58]. A working intestinal model should enable consistent control over the growth rate of both mammalian and microbial cell populations in order to realistically mimic the host intestine. With this proviso in mind, Kim et al. [33] developed a protocol for culturing host cells and commensal bacteria in a microfluidic device. Using pneumatically-controlled trapping, they were able to hold and segregate the different cell types, creating bacterial “islands” of E. coli surrounded by HeLa cells, with separate inlet and outlet ports for providing growth media and removing waste. Additionally, they were able to use this device to study the attachment and proliferation of model pathogens (enterohemorrhagic E. coli) onto HeLa cells, making studies more realistic due to the added presence of commensal bacteria. They envisaged that this model can be used for screening pre and pro-biotic strains, as well as investigating the role of specific pathogenic infectious signals in intestinal disorders.

By using more complicated microfluidic approaches, Kim et al. [32] created an “gut on a chip” device that enabled the co-culture of Caco-2 cells and Lactobacillus rhamnosus GG (LGG) on a porous membrane, with fluid flow channels for sustained cell culture and cyclic strain for mimicking peristaltic motions. Using a combination of immunofluorescence, enzyme assays and TEER measurement, they found that

cyclic strain caused an increase in Caco-2 elongation, differentiation and paracellular permeability. Additionally, they found that the LGG cells remained adherent for 1 week, and that the addition of the microbes actually increased tight junction formation, as shown through TEER analysis. They theorized that fluid flow movement accompanied by peristaltic motions prevents the accumulation and overgrowth of microbes that might otherwise affect the viability of intestinal cells, by enabling the removal of unattached/dead cells and harmful organic acids.

As well as providing a platform for the study of host-microbial interactions, small intestinal models can potentially aid in the study of gene transfer in the gut. The transfer of antibiotic resistance genes between intestinal microbes can have a dramatic effect on both the ecology and evolution of the microbial population, particularly as acquired genes may be advantageous, allowing colonization of otherwise hostile niches and/or improved pathogenicity. This can have serious detrimental effects on human health, leading to chronic, poorly treatable infections [61]. In recent years, much of the research into microbial conjugation in the gut has been focused on in vivo experiments in animals. Bacterial donors and recipients have been cultured in vitro, followed by inoculating directly into live animals and then subsequent detection through faecal matter or animal sacrifice [4]. However, in addition to being expensive and unreliable, live animal models make it difficult to observe and document plasmid transfer and gene acquisitions as they occur in real time. In vitro small intestinal models are small scale, yet they may enable us to answer questions from which previous research has elicited conflicting data. For example, Feld et al. [20] found a

higher rate of transfer in gnotobiotic rats than on filters suggesting that the gut environment facilitates transfer relative to filter matings; whereas Licht et al. [40] concluded that in the mouse gut only a small proportion of the bacteria exchange DNA near the epithelial cells perhaps because they behave more like an unmixed biofilm. Emulating the physical and cellular make-up of our intestines could therefore create an opportunity to answer these questions more fully, and be a major breakthrough in the study of antibiotic resistance and chemical communication between bacteria and epithelia.

CONCLUSIONS

Since firstly invented more than two decades ago, in vitro small intestinal models have been extremely useful in predicting drug oral absorption efficiency as well as understanding small intestinal epithelium differentiation and functionality. Benefited by recent developments in stem cell and microfabrication techniques, better in vitro models with physiologically relevant small intestinal strucutres as well as excellular microenvironments are being realized. Since we still know little about GI host-microbial interactions, accurate in vitro small intestinal models could be a cutting-edge tool to explore this area and possibly provide therapies for intestine-related diseases.

ACKNOWLEDGEMENTS

This work was funded by The Hartwell Foundation (Collaborative Grant) and the National Institutes of Health (DP2 New Innovator).

REFERENCE

1. Abbott A (2003) Cell culture: Biology's new dimension. Nature 424:870-872

2. Ahlman H, Nilsson O (2001) The gut as the largest endocrine organ in the body. Annals of Oncology 12:S63-S68

3. Artursson P, Palm K, Luthman K (2001) Caco-2 monolayers in experimental and theoretical predictions of drug transport. Advanced Drug Delivery Reviews 46:27-43

4. Avrain L, Vernozy-Rozand C, Kempf I (2004) Evidence for natural horizontal transfer of tetO gene between Campylobacter jejuni strains in chickens. Journal of Applied Microbiology 97:134-140

5. Baker M (2011) Tissue models: A living system on a chip. Nature 471:661-665

6. Barker N, Van De Wetering M, Clevers H (2008) The intestinal stem cell. Genes & Development 22:1856-1864

7. Benoit YD, Paré F, Francoeur C, Jean D, Tremblay E, Boudreau F, Escaffit F, Beaulieu J-F (2010) Cooperation between HNF-1α, Cdx2, and GATA-4 in initiating an enterocytic differentiation program in a normal human intestinal epithelial progenitor cell line. American Journal of Physiology - Gastrointestinal and Liver Physiology 298:G504-G517

8. Bernet MF, Brassart D, Neeser JR, Servin AL (1994) Lactobacillus acidophilus LA 1 binds to cultured human intestinal cell lines and inhibits cell attachment and cell invasion by enterovirulent bacteria. Gut 35:483-489

9. Brovko L, Minikh O, Piekna A, Griffiths MW (2011) Bioluminescent high-throughput assay for the bacteria adherence to the tissue culture cells. Biotechnology and Bioengineering 108:1628-1633

10. Brown RA, Phillips JB (2007) Cell responses to biomimetic protein scaffolds used in tissue repair and engineering. International Review of Cytology - a Survey of Cell Biology, Vol 262 262:75-150

11. Buchan AMJ (1999) III. Endocrine cell recognition of luminal nutrients. American Journal of Physiology - Gastrointestinal and Liver Physiology 277:G1103-G1107

12. Carroll KM, Wong TT, Drabik DL, Chang EB (1988) Differentiation of rat small intestinal epithelial cells by extracellular matrix. American Journal of Physiology - Gastrointestinal and Liver Physiology 254:G355-G360

13. Cruz N, Qi L, Alvarez X, Berg RD, Deitch EA (1994) The Caco-2 cell monolayer system as an in vitro model for studying bacterial-enterocyte interactions and bacterial translocation. Journal of Burn Care and Rehabilitation 15:207-212

14. Cukierman E, Pankov R, Stevens DR, Yamada KM (2001) Taking cell-matrix adhesions to the third dimension. Science 294:1708-1712

15. Danielsen E, Hansen G (2008) Lipid raft organization and function in the small intestinal brush border. Journal of Physiology and Biochemistry 64:377-382

16. Darfeuille-Michaud A, Boudeau J, Bulois P, Neut C, Glasser AL, Barnich N, Bringer MA, Swidsinski A, Beaugerie L, Colombel JF (2004) High prevalence of adherent-invasive Escherichia coli associated with ileal mucosa in Crohn's disease. Gastroenterology 127:412-421

17. Dharmani P, Srivastava V, Kissoon-Singh V, Chadee K (2009) Role of intestinal mucins in innate host defense mechanisms against pathogens. Journal of Innate Immunity 1:123-135

18. Diamond JM, Karasov WH (1987) Adaptive regulation of intestinal nutrient transporters. Proceedings of the National Academy of Sciences 84:2242-2245

19. Drucker DJ, Jin T, Asa SL, Young TA, Brubaker PL (1994) Activation of proglucagon gene transcription by protein kinase-A in a novel mouse enteroendocrine cell line. Molecular Endocrinology 8:1646-1655

20. Feld L, Schjørring S, Hammer K, Licht TR, Danielsen M, Krogfelt K, Wilcks A (2008) Selective pressure affects transfer and establishment of a Lactobacillus plantarum resistance plasmid in the gastrointestinal environment. Journal of Antimicrobial Chemotherapy 61:845-852

21. Ferain E, Legras R (2003) Track-etch templates designed for micro- and nanofabrication. Nuclear Instruments and Methods in Physics Research Section B: Beam Interactions with Materials and Atoms 208:115-122

22. Gerard J. Tortora SRG (1999) Principles of Anatomy and Physiology. John Wiley & Sons Inc

23. Gribble FM, Williams L, Simpson AK, Reimann F (2003) A novel glucose-sensing mechanism contributing to glucagon-like peptide-1 secretion from the GLUTag cell line. Diabetes 52:1147-1154

24. Griffith LG, Swartz MA (2006) Capturing complex 3D tissue physiology in vitro. Nat Rev Mol Cell Biol 7:211-224

25. Hidalgo IJ, Li J (1996) Carrier-mediated transport and efflux mechanisms in Caco-2 cells. Advanced Drug Delivery Reviews 22:53-66

26. Hidalgo IJ, Raub TJ, Borchardt RT (1989) Characterization of the human colon carcinoma cell line (Caco-2) as a model system for intestinal epithelial permeability. Gastroenterology 96:736-749

27. Hilgers AR, Conradi RA, Burton PS (1990) Caco-2 cell monolayers as a model for drug transport across the intestinal mucosa. Pharmaceutical Research 7:902-910

28. Höfer D, Asan E, Drenckhahn D (1999) Chemosensory perception in the gut. Physiology 14:18-23

29. Irvine JD, Takahashi L, Lockhart K, Cheong J, Tolan JW, Selick HE, Grove JR (1999) MDCK (Madin–Darby canine kidney) cells: A tool for membrane permeability screening. Journal of Pharmaceutical Sciences 88:28-33

30. Katsuma S, Hirasawa A, Tsujimoto G (2005) Bile acids promote glucagon-like peptide-1 secretion through TGR5 in a murine enteroendocrine cell line STC-1. Biochemical and Biophysical Research Communications 329:386-390

31. Kernéis S, Bogdanova A, Kraehenbuhl J-P, Pringault E (1997) Conversion by Peyer's patch lymphocytes of human enterocytes into M cells that transport bacteria. Science 277:949-952

32. Kim HJ, Huh D, Hamilton G, Ingber DE (2012) Human gut-on-a-chip inhabited by microbial flora that experiences intestinal peristalsis-like motions and flow. Lab on a Chip 12:2165-2174

33. Kim J, Hegde M, Jayaraman A (2010) Co-culture of epithelial cells and bacteria for investigating host-pathogen interactions. Lab on a Chip 10:43-50

34. Kim Y, Ho S (2010) Intestinal goblet cells and mucins in health and disease: recent insights and progress. Current Gastroenterology Reports 12:319-330

35. Kleerebezem M, Vaughan EE (2009) Probiotic and gut lactobacilli and bifidobacteria: molecular approaches to study diversity and activity. Annual Review of Microbiology 63:269-290

36. Laparra JM, Sanz Y (2009) Comparison of in vitro models to study bacterial adhesion to the intestinal epithelium. Letters in Applied Microbiology 49:695-701

37. Lee Y-K, Puong K-Y, Ouwehand AC, Salminen S (2003) Displacement of bacterial pathogens from mucus and Caco-2 cell surface by lactobacilli. Journal of Medical Microbiology 52:925-930

38. Lesuffleur T, Barbat A, Dussaulx E, Zweibaum A (1990) Growth adaptation to methotrexate of HT-29 human colon carcinoma cells is associated with their ability to differentiate into columnar absorptive and mucus-secreting cells. Cancer Research 50:6334-6343

39. Ley RE, Peterson DA, Gordon JI (2006) Ecological and evolutionary forces shaping microbial diversity in the human intestine. Cell 124:837-848

40. Licht TR, Christensen BB, Krogfelt KA, Molin S (1999) Plasmid transfer in the animal intestine and other dynamic bacterial populations: the role of community structure and environment. Microbiology 145:2615-2622

41. Linnankoski J, Mäkelä J, Palmgren J, Mauriala T, Vedin C, Ungell A-L, Lazorova L, Artursson P, Urtti A, Yliperttula M (2010) Paracellular porosity and pore size of the human intestinal epithelium in tissue and cell culture models. Journal of Pharmaceutical Sciences 99:2166-2175

42. Liu H, Roy K (2005) Biomimetic three-dimensional cultures significantly increase hematopoietic differentiation efficacy of embryonic stem cells. Tissue engineering 11:319-330

43. Lussier CR, Babeu J-P, Auclair BA, Perreault N, Boudreau F (2008) Hepatocyte nuclear factor-4α promotes differentiation of intestinal epithelial cells in a coculture system. American Journal of Physiology - Gastrointestinal and Liver Physiology 294:G418-G428

44. Mahler GJ, Esch MB, Tako E, Southard TL, Archer SD, Glahn RP, Shuler ML (2012) Oral exposure to polystyrene nanoparticles affects iron absorption. Nat Nano 7:264-271

45. Mahler GJ, Shuler ML, Glahn RP (2009) Characterization of Caco-2 and HT29-MTX cocultures in an in vitro digestion/cell culture model used to predict iron bioavailability. The Journal of Nutritional Biochemistry 20:494-502

46. Manning AP, Thompson WG, Heaton KW, Morris AF (1978) Towards positive diagnosis of the irritable bowel. BMJ 2:653-654

47. Moon HW (1978) Mechanisms in the pathogenesis of diarrhea: a review. Journal of the American Veterinary Medical Association 172:443-448

48. Murray JA (1999) The widening spectrum of celiac disease. American Journal of Clinical Nutrition 69:354-365

49. Nutten S, Sansonetti P, Huet G, Bourdon-Bisiaux C, Meresse B, Colombel J-F, Desreumaux P (2002) Epithelial inflammation response induced by Shigella flexneri depends on mucin gene expression. Microbes and Infection 4:1121-1124

50. Olson H, Betton G, Robinson D, Thomas K, Monro A, Kolaja G, Lilly P, Sanders J, Sipes G, Bracken W, Dorato M, Van Deun K, Smith P, Berger B, Heller A (2000) Concordance of the toxicity of pharmaceuticals in humans and in animals. Regulatory Toxicology and Pharmacology 32:56-67

51. Perreault N, Beaulieu J-F (1996) Use of the dissociating enzyme thermolysin to generate viable human normal intestinal epithelial cell cultures. Experimental Cell Research 224:354-364

52. Pinto M, Appay, M. D., Simon-Assmann, P., Chevalier, G., Dracopoli, N., Fogh, J., and Zweibaum, A. (1982) Enterocytic differentiation of cultured human colon cancer cells by replacement of glucose by galactose in the medium. Biology of the cell 44:193-196

53. Pinto M, Robine-Leon, S., Appay, Md, Kedinger, M., Triadou, N., Dussaulx, I'.. Lacroix, B.,, Simon-Assmann PH, K., Fogh, J., and Zweibaum, A (1983) Enterocyte-like differentiation and polarization of the human colon carcinoma cell line Caco-2 in culture biology of the cell 47

54. Pusch J, Votteler M, Göhler S, Engl J, Hampel M, Walles H, Schenke-Layland K (2011) The physiological performance of a three-dimensional model that mimics the microenvironment of the small intestine. Biomaterials 32:7469-7478

55. Quaroni A, Hochman J (1996) Development of intestinal cell culture models for drug transport and metabolism studies. Advanced Drug Delivery Reviews 22:3-52

56. Quaroni A, Wands J, Trelstad RL, Isselbacher KJ (1979) Epithelioid cell cultures from rat small intestine. Characterization by morphologic and immunologic criteria. The Journal of Cell Biology 80:248-265

57. Quastler H, Sherman FG (1959) Cell population kinetics in the intestinal epithelium of the mouse. Experimental Cell Research 17:420-438

58. Quigley EMM, Quera R (2006) Small intestinal bacterial overgrowth: roles of antibiotics, prebiotics, and probiotics. Gastroenterology 130:S78-S90

59. Resta-Lenert S, Barrett KE (2003) Live probiotics protect intestinal epithelial cells from the effects of infection with enteroinvasive Escherichia coli (EIEC). Gut 52:988-997

60. Rindi G, Grant SGN, Yiangou Y, Ghatei MA, Bloom SR, Bautch VL, Solcia E, Polak JM (1990) Development of neuroendocrine tumors in the gastrointestinal tract of transgenic mice. Heterogeneity of hormone expression. The American Journal of Pathology 136:1349–1363

61. Salyers AA, Gupta A, Wang Y (2004) Human intestinal bacteria as reservoirs for antibiotic resistance genes. Trends in Microbiology 12:412-416

62. Sato T, Vries RG, Snippert HJ, Van De Wetering M, Barker N, Stange DE, Van Es JH, Abo A, Kujala P, Peters PJ, Clevers H (2009) Single Lgr5 stem cells build crypt–villus structures in vitro without a mesenchymal niche. Nature 459:262-265

63. Schmeichel KL, Bissell MJ (2003) Modeling tissue-specific signaling and organ function in three dimensions. Journal of Cell Science 116:2377-2388

64. Sidhu SS, Thompson DG, Warhurst G, Case RM, Benson RSP (2000) Fatty acid-induced cholecystokinin secretion and changes in intracellular Ca2+ in two enteroendocrine cell lines, STC-1 and GLUTag. The Journal of Physiology 528:165-176

65. Skovbjerg H (1981) Immunoelectrophoretic studies on human small intestinal brush border proteins—the longitudinal distribution of peptidases and disaccharidases. Clinica Chimica Acta 112:205-212

66. Smirnova MG, Guo L, Birchall JP, Pearson JP (2003) LPS up-regulates mucin and cytokine mRNA expression and stimulates mucin and cytokine secretion in goblet cells. Cellular Immunology 221:42-49

67. Spence JR, Mayhew CN, Rankin SA, Kuhar MF, Vallance JE, Tolle K, Hoskins EE, Kalinichenko VV, Wells SI, Zorn AM, Shroyer NF, Wells JM (2011) Directed differentiation of human pluripotent stem cells into intestinal tissue in vitro. Nature 470:105-109

68. Sternini C, Anselmi L, Rozengurt E (2008) Enteroendocrine cells: a site of 'taste' in gastrointestinal chemosensing. Current Opinion in Endocrinology, Diabetes and Obesity 15:73-78

69. Sun D, Lennernas H, Welage LS, Barnett JL, Landowski CP, Foster D, Fleisher D, Lee K-D, Amidon GL (2002) Comparison of human duodenum and Caco-2 gene expression profiles for 12,000 gene sequences tags and correlation with permeability of 26 drugs. Pharmaceutical Research 19:1400-1416

70. Sung JH, Yu J, Luo D, Shuler ML, March JC (2011) Microscale 3-D hydrogel scaffold for biomimetic gastrointestinal (GI) tract model. Lab on a Chip 11:389-392

71. Tavelin S, Taipalensuu J, Hallböök F, Vellonen K-S, Moore V, Artursson P (2003) An improved cell culture model based on 2/4/A1 cell monolayers for studies of intestinal drug transport: characterization of transport routes. Pharmaceutical Research 20:373-381

72. Van Der Flier LG, Clevers H (2009) Stem cells, self-renewal, and differentiation in the intestinal epithelium. Annual Review of Physiology 71:241-260

73. Walter E, Janich S, Roessler BJ, Hilfinger JM, Amidon GL (1996) HT29-MTX/Caco-2 cocultures as an in vitro model for the intestinal epithelium: In vitro–in vivo correlation with permeability data from rats and humans. Journal of Pharmaceutical Sciences 85:1070-1076

74. Wikman-Larhed A, Artursson P (1995) Co-cultures of human intestinal goblet (HT29-H) and absorptive (Caco-2) cells for studies of drug and peptide absorption. European Journal of Pharmaceutical Sciences 3:171-183

75. Wu SV, Rozengurt N, Yang M, Young SH, Sinnett-Smith J, Rozengurt E (2002) Expression of bitter taste receptors of the T2R family in the gastrointestinal tract and enteroendocrine STC-1 cells. Proceedings of the National Academy of Sciences 99:2392-2397

76. Yoshida S, Kajimoto Y, Yasuda T, Watada H, Fujitani Y, Kosaka H, Gotow T, Miyatsuka T, Umayahara Y, Yamasaki Y, Hori M (2002) PDX-1 Induces Differentiation of Intestinal Epithelioid IEC-6 Into Insulin-Producing Cells. Diabetes 51:2505-2513

77. Yu J, Peng S, Luo D, March JC (2012) In vitro 3D human small intestinal villous model for drug permeability determination. Biotechnology and Bioengineering 109:2173-2178

CHAPTER TWO:

MICROSCALE 3D HYDROGEL SCAFFOLD FOR BIOMIMETIC GASTROINTESTINAL (GI) TRACT MODEL

Sung JH [‡ac], Yu J [‡a], Luo D [a], Shuler ML [b], March JC [*a] (2011) Microscale 3-D hydrogel scaffold for biomimetic gastrointestinal (GI) tract model. Lab on a Chip 11:389-392 - Reproduced by permission of The Royal Society of Chemistry

[a] Biological and Environmental Engineering, Cornell University, USA.
[b] Biomedical Engineering, Cornell University, USA
[c] Department of Chemical Engineering, Hongik University, Seoul, Korea
[‡] These authors contributed equally.

ABSTRACT

Here we describe a simple and efficient method for fabricating natural and synthetic hydrogels into 3D geometries with high aspect ratio and curvature. Fabricating soft hydrogels into such shapes using conventional techniques has been extremely difficult. Combination of laser ablation and sacrificial molding technique using calcium alginate minimizes the stress associated with separating the mold from the hydrogel structure, and therefore allows fabrication of complex structures without damaging them. As a demonstration of this technique, we have fabricated a microscale collagen structure mimicking the actual density and size of human intestinal villi. Colon carcinoma cell line, Caco-2 cells, were seeded onto the structure and cultured for 3 weeks until the whole structure was covered, forming finger-like structures mimicking the intestinal villi covered with epithelial cells. This method will enable construction of in vitro tissue models with physiologically-realistic geometries in at microscale resolutions.

INTRODUCTION

3D hydrogel cell cultures have been of a great interest in biomedical engineering recently [1, 7]. Culturing cells in 3-dimensional space has been shown to provide cells with a more physiologically realistic environment, including cell-to-cell and cell-to-matrix interactions and proper chemical and mechanical signaling. Adequate 3D cues allow cells to exhibit more authentic functions, compared to traditional 2D cell cultures, which are known to be significantly different from their in vivo counterparts. As the importance of 3D cell culture is growing, various hydrogels have been developed as scaffolds for 3D cell culture. Hydrogels are hydrophilic polymers, with

their major fraction being water, and thus provide a cell-friendly environment as well as mechanical support for cell growth and differentiation. A large number of synthetic and naturally derived hydrogels exist, with a wide range of mechanical and chemical properties [23]. Typically, cells are encapsulated within or cultured on the surface of these hydrogels. For cell-laden hydrogels to correctly reproduce the biological functions of in vivo tissues, it is important to accurately mimic the 3D geometry of the native tissue in micro/nanometre resolution [11, 13, 15, 22].

For this reason, microscale fabrication of hydrogel structures has been of a great interest in biomedical applications, and several methods have been developed that enable synthesizing hydrogels with controlled features [12, 27]. The most well-known methods include replica molding, photo-polymerization, and direct printing [12, 25, 27]. While these methods can control the feature size to microscale resolutions, they are typically limited to the fabrication of low to medium aspect ratio structures, with perpendicular shapes. It is technically challenging to fabricate more complex structures, such as a structure with a high aspect ratio or a curvature, which are frequently encountered in nature. Examples include long bundles in native skeletal muscles [4] and the villi structure lining the apical side of the gastrointestinal (GI) tract [29]. Conventional replica molding is not suitable for fabrication of such shapes, since an attempt to separate the soft hydrogel scaffold from a mold would easily result in destruction of the structure. While the photo-polymerization method has a resolution of several micrometers, it cannot create curved 3D shapes, and is limited to photo-polymerizable hydrogels only [21]. Direct printing methods can be used for

free-form fabrication of arbitrary shapes, but are typically suitable for low-resolution applications (hundreds of micrometers), cannot make curved shapes, and require expensive equipments [10, 16].

In this study, we report a novel method for fabrication of 3D structures made from soft hydrogels. Laser ablation creates a controlled array of deep holes in a plastic mold, which is used to make a Poly (dimethyl sulfoxane) (PDMS) mold with the desired features. The PDMS mold is used to create a secondary mold made of calcium alginate, which is subsequently dissolved after forming a 3D structure with the final hydrogel (Figure 2.1). Using calcium alginate as a sacrificial mold eliminates the need for applying force for separation of the hydrogel structure, and enables creation of a hydrogel scaffold with a high aspect ratio and curvature. As a demonstration of this technique's feasibility, we have fabricated a collagen scaffold mimicking the 3D geometry of gastrointestinal tract villi. Then we cultured Caco-2 cells , human epithelial colorectal adenocarcinoma cells , on the scaffold for three weeks, which resulted in cell-coated hydrogel villi with a striking similarity to the human jejunal villi (Figure 2.5 and 2.7). The novelty of this method lies in the use of alginate hydrogel for sacrificial molding under physiological conditions (pH, temperature). These steps enable creation of high aspect ratios and the use of “cell-friendly” hydrogels that would be unstable at higher temperatures or non-physiological pH.

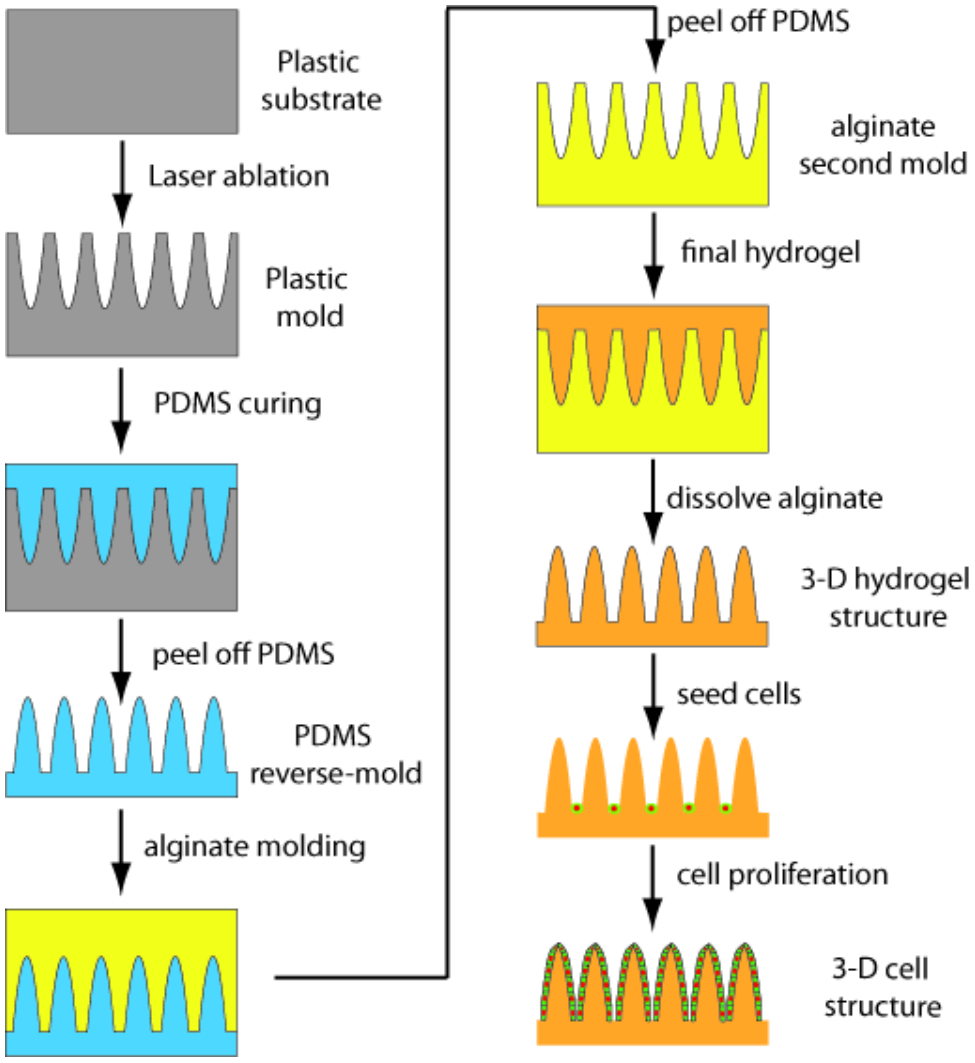

Figure 2.1 Overall fabrication process. The first plastic mold is created by laser ablation, from which the PDMS reverse-mold is created. The alginate second mold is made from the PDMS, and dissolved after the final hydrogel structure is made.

MATERIALS AND METHODS

Laser ablation and PDMS mold fabrication

Poly (methyl methacrylate) (PMMA) was purchased from Ithaca plastics Inc (Ithaca, NY). The UV laser micromachining system Resonetics Maestro 1000 (Resonetics, Nashua, NH) was used to fabricate high-aspect ratio holes in PMMA [14]. The laser energy was stabilized at 50 mJ by using the energy stable function. A stainless sheet with 4 mm diameter circle was used as laser shutter. The laser pulse rate was set at 75PPS (pulse per second), and the pulse number was set to 1100. At these parameters, the depth of hole was estimated to be approximately 506 um, which was later confirmed by confocal microscopy. The distance between rows and columns was set to be 200 μm for 25 holes/mm^2 density. To measure the depth of hole, a drilled PMMA sheet was coated with gold by a gold sputtering system (Polaron) for 30 min to generate detectable signals. The depth was measured by Wyko HD-3300 noncontact surface height measurement system (Veeco Instruments Inc, Tucson, AZ). A linear relationship was found between laser pulse number and hole depth (Figure 2.3). PDMS monomer and curing agent (Sylgard 184, Dow Corning, Midland, MI) were mixed at 7:1 ratio, and poured onto the PMMA with holes. After degassing to remove bubbles and ensure the PDMS prepolymer solution filled up the holes, PDMS was cured at room temperature overnight. After curing, the PDMS mold was slowly peeled off.

Surface coating of PDMS villous scaffold

PDMS scaffold was treated by oxygen plasma (Harrick Plasma, Ithaca, NY) for 60 seconds. Right after plasma treating, PDMS scaffold was coated with 200μg/ml type I collagen (BD Biosciences, San Jose, CA) in 0.02N acetic acid for 2 hours in 37 °C incubator. After coating, PDMS scaffold was washed by PBS buffer for 3 times and kept in 4 °C until use.

Cell culture

Caco-2 cells (ATCC, Manassas, VA) were maintained in Dulbecco's Modified Eagle's Media (DMEM, Cellgro, Manassas, VA), with 10% fetal bovine serum (FBS, Invitrogen, Carlsbad, CA) and 1X anti-biotic anti-mycotic (Invitrogen). Human mesenchymal stem cells (hMSCs, Lonza, Basel, Switzerland) were maintained in mesenchymal stem cell growth medium (Lonza). Rat small intestinal epithelial crypt cells IEC-6 Cdx2 HNF4-α (a kind gift from Professor François Boudreau, Universite´ de Sherbrooke) were maintained in DMEM containing 0.1 U/ml insulin, 4.5 g/l D-glucose, 25 mM HEPES, 1% penicillin-streptomycin and 10% FBS. For co-culture, Human mesenchymal stem cells were cultured on PDMS scaffold for 14 days, then IEC-6 Cdx2 HNF4-α cells were seeded on top at 1×10^5 cells/cm^2 seeding density. After seeding, cells were maintained in co-culture media, which contained DMEM with 0.1 U/ml insulin, 4.5 g/l D-glucose, 25 mM HEPES, 1% penicillin-streptomycin, 10% FBS and 50 μg/ml ascorbic acid. The media was replaced every 2 days during the culture.

Fabrication of alginate mold and collagen/PEG-DA scaffold

For fabrication of an alginate mold, a PDMS stamp with villi structure was made first. An aluminum gasket rig was designed based on the previously reported method using a gasket for fabricating microfluidic channels in calcium alginate[6]. It consists of a base frame (G1) with a recess (7mm x 7mm, 0.7 mm depth), a middle frame for holding PDMS (G2), and the top frame (G3). The three frames were secured with screws. The PDMS stamp was cured overnight at room temperature to avoid deformation of aluminum from heating. After curing, G1 was removed, and the PDMS villi structure (made from the PMMA mold) was glued on top of the cured PDMS. Uncured PDMS prepolymer solution was used as glue. The rig was left at room temperature overnight until the PDMS glue set. After the PDMS villi piece was fully glued, an aluminum gasket (G4) was secured on top of the PDMS stamp. G4, a square piece with a 10 mm by 10 mm hole, is used as a gasket for holding the alginate mold. Sterile-filtered 2.5% sodium alginate (10/60 sodium alginate, FMC biopolymer, Philadelphia, PA) was inserted into hole in G4. The top was covered with a polycarbonate membrane (G5, 8 μm pore size, 25 mm diameter, Fisher Scientific, Pittsburg, PA) and a perforated aluminum piece (G6) with 1mm diameter holes. An aluminum gasket (G7), which works as a reservoir for calcium chloride solution is secured on top, and 3 ml of 60 mM calcium chloride solution was inserted into the reservoir. After incubating at room temperature for 4 hours, a gasket with alginate mold (G4) was separated from other gasket pieces. Collagen or PEG-DA pre-gel solution (5 mg/ml final concentration in 0.1% acetic acid for collagen and 20% (w/v) for PEG-DA with 0.5% 2,2'-Azobis(2-methylpropionamidine) dihydrochloride as a

photoinitiator) was placed in the alginate mold. Collagen pre-gel solution was neutralized with 1M NaOH and kept in ice before the insertion. Collagen was gelled by raising the temperature to 37 °C, and PEG-DA was polymerized by exposure to UV for 30 minutes in a UV crosslinker (Spectronics Corporation, Westbury, NY). The collagen was further crosslinked with 0.1% glutaraldehyde for 4 hours. After the gel was made, the alginate mold was dissolved using 60 mM EDTA solution for 3 hours at room temperature. The whole process is summarized in Figure 2.2.

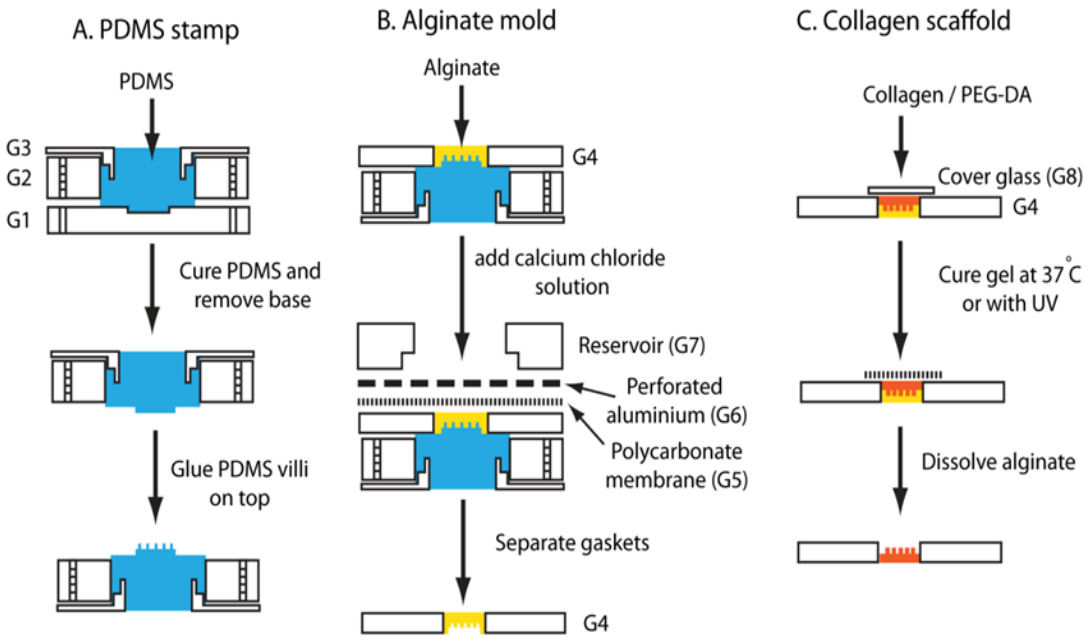

Figure 2.2 Summary of fabrication process. A PDMS stamp holds the PDMS villi structure on top, where sodium alginate is placed and cured with a calcium chloride solution. After curing alginate, collagen is inserted into the alginate mold and crosslinked. The sacrificial alginate mold is later dissolved with an EDTA solution.

Cell seeding and cell staining on collagen scaffolds

After fabrication, collagen scaffold was incubated in 5% L-glutamic acid for 48 hours at room temperature to reduce the cytotoxicity of glutaraldehyde and restore the biocompatibility [9]. Then the scaffold was washed in PBS three times, and incubated in PBS until cell seeding. After trypsinization, live cells were counted and cells were resuspended in fresh medium to the final concentration of $1x10^5$~$5x10^5$ cells/ml. A drop of cell suspension was placed on top of the collagen scaffold and incubated for 30 minutes before medium was added. After cell seeding, the collagen scaffold was maintained in a cell culture incubator with the medium changed every two days. Depending on the initial seeding density, cells will cover the collagen scaffold in 7~10 days. After the collagen scaffold was covered, cells were fixed with formaldehyde, washed with PBS, and then stained with Alexa Fluor 488 phalloidin(Invitrogen) and TO-PRO-3 (Invitrogen). Fluorescently labeled phalloidin is a high-affinity probe for F-actin and TO-PRO-3 is a nucleic acid stain. Confocal images were taken with Leica SP2 confocal microscope (Leica Microsystems, Bannockburn, IL) and 3D image was rendered using Volocity (Perkinelmer, Waltham, MA). To maintain sterility, all gasket pieces were autoclaved prior to use and the gasket assembly and cell seeding was done in biosafety cabinet.

RESULTS

Fabrication of PMMA mold, PDMS villi and hydrogel scaffolds

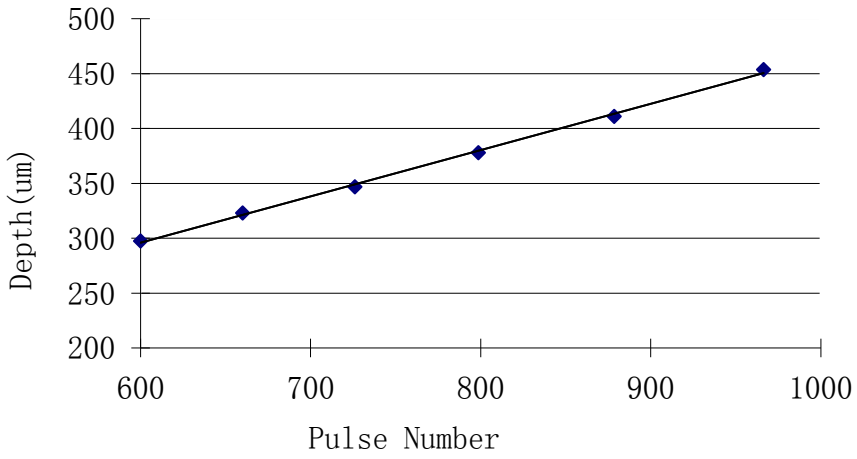

Figure 2.3 Measured depth of holes in PMMA vs. laser pulse number

Laser ablation was used to create an array of holes on a plastic mold. By controlling the pulse rate and the pulse number of the laser, it was possible to control the depth of the holes to be approximately 500 micrometer (Figure 2.3). The density and the depth of the holes were based on the actual density and the geometry of the human GI tract [26]. The bright-field microscope images of the fabricated plastic mold, the PDMS villi, alginate second mold, and the final collagen scaffold are shown in the Figure 2.4.

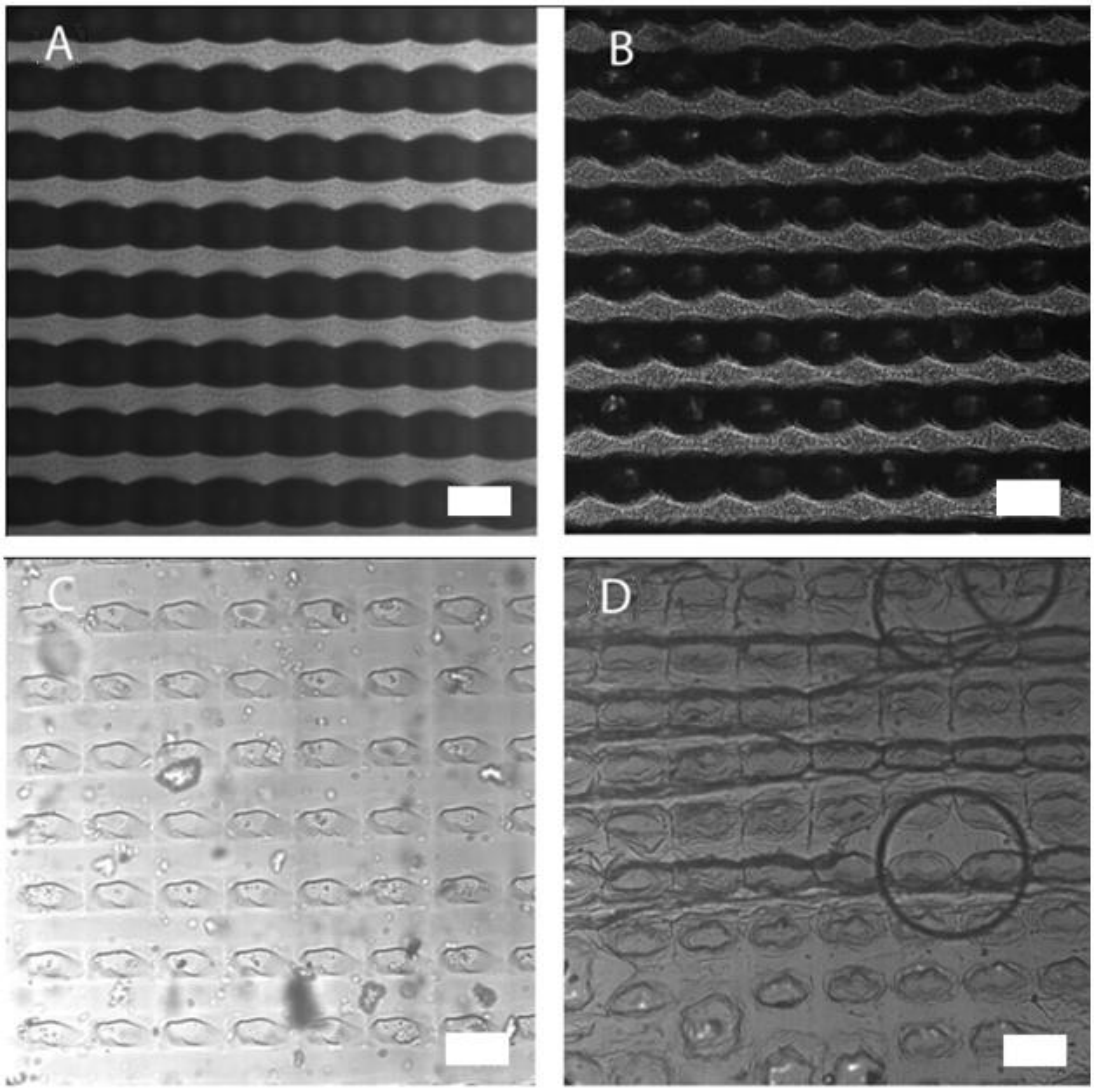

Figure 2.4 (A) PMMA surface with holes. There are 25 holes in 1mm^2. Each hole has oval shape due to the melting effect of laser. The longer axis of the oval is about 200 µm, and the shorter axis is about 160 µm. (B) PDMS surface with villi structures (C) Alginate mold with holes (D) Collagen scaffold with villi structures. The scale bars are 0.2mm.

Curing PDMS on the plastic mold and peeling off the PDMS resulted in PDMS villi structures. As can be seen in Figure 2.5A, the PDMS villi faithfully reproduced the

originally intended geometry. Using the PDMS villi as the base template, an alginate gel was formed on the PDMS villi and separated to create the secondary mold. For this process, a custom-designed aluminium gasket was made to hold the hydrogels tightly against the PDMS villi (Figure 2.2). This gasket also minimized deformation of the alginate mold during gelling, and allowed precise control of the thickness of the alginate and final hydrogel structures. 2.5–4% alginate was used, which was sufficiently rigid to allow easy separation of the alginate mold from the PDMS villi. The alginate mold consists of an array of holes, with the same geometry as the original plastic mold, which also makes it easier to separate without destruction of the features.

For the final hydrogels, two types of hydrogels were used, collagen and polyethylene glycol diacrylate (PEG-DA), which are one of the most widely used natural and synthetic hydrogels for cell culture, respectively. Collagen is the most abundant protein in mammals, and is frequently used as a scaffold for cultures of various cell types [24]. PEG-DA is a synthetic, biocompatible hydrogel widely used for hydrogel cell culture [3]. Figure 2.5B shows an image of a typical structure made with 0.5% (w/v) collagen. Figure 2.5C shows the same structure made in 20% PEG-DA. In both cases, the height of the structure was about 450–500 mm, and the aspect ratio was close to 5. This verifies that the serial molding process replicates the 3D geometry accurately.

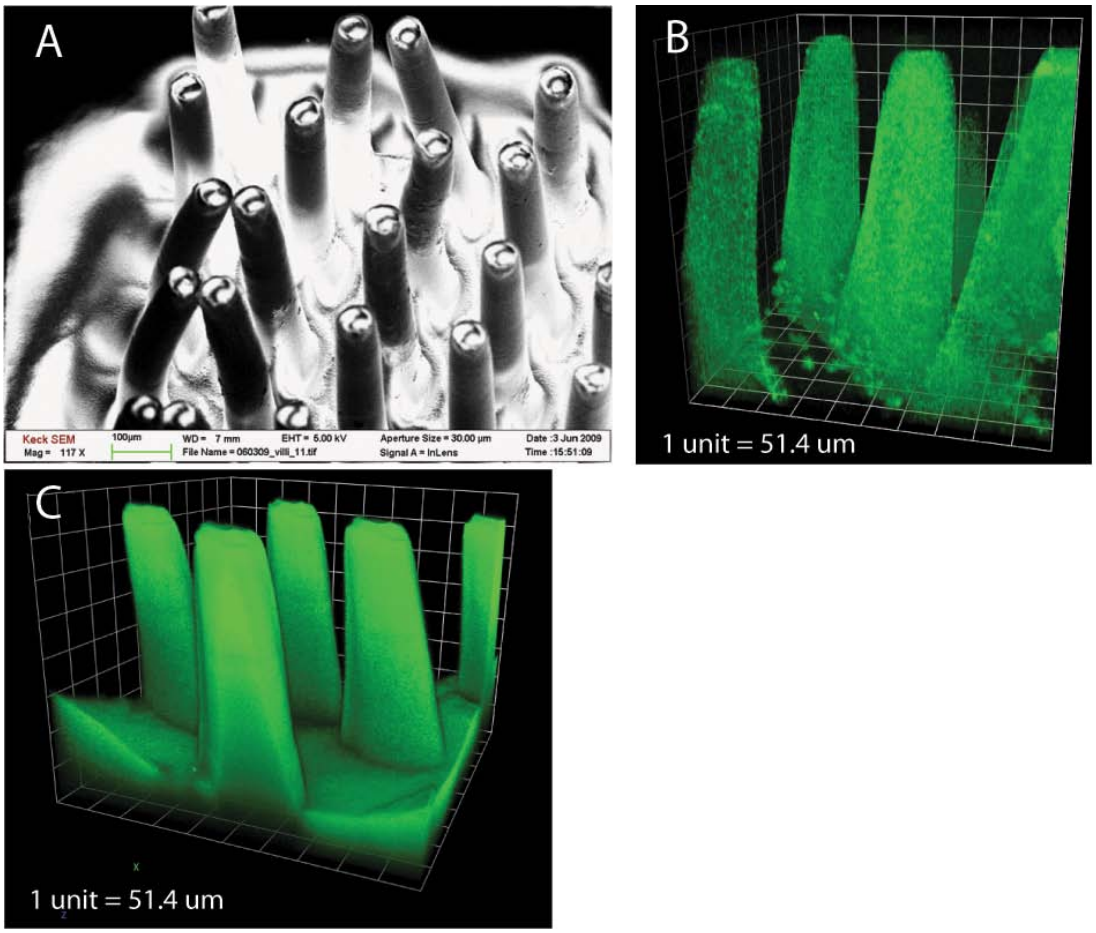

Figure 2.5 (A) SEM image of the PDMS villi structure. (B) Confocal microscope image of the collagen scaffold after 3D rendering. (C) Confocal microscope image of the PEG scaffold after 3D rendering.

Cell culture on PDMS villous scaffold

To demonstrate using the villi structure as a 3D scaffold for cell culture, we selected the Caco-2 cell line, which originated from human colon carcinoma, and is widely used as an in vitro model of gastrointestinal epithelial cell lining in drug absorption studies [2]. Caco-2 cells were seeded onto collagen coated PDMS villous scaffold first. After 4 days of culture, Caco-2 cells proliferated from the bottom to the half

height of the PDMS villus (Figure 2.6A). After 7 days of culture, Caco-2 cells covered the whole villus structure and reached confluency (Figure 2.6B), forming a differentiated cell morphology near the tip of villus (Figure 2.6D). On the 12^{th} day of culture, higher cell density was observed on PDMS villus (Figure 2.6C). However, after 12 days of culture, Caco-2 cells failed to continue differentiating and detached from the PDMS villus.

Apart from Caco-2 cell line, a co-culture system was also tested on the PDMS villous scaffold. Human mesenchymal stem cells (hMSCs) were seeded onto PDMS villi and cultured for 14 days to mimic the mesenchymal layer under the small intestine epithelia [18]. Similarly to the Caco-2 cell line, hMSCs covered the whole villus structure after 7 days of culture (Figure 2.6E). IEC-6 Cdx2 HNF4-α cells promptly covered the whole hMSCs layer after being co-cultured on top of the hMSCs for 4 days (Figure 2.6F). However, both cell lines began to detach from the PDMS villus and failed to continue differentiating during longer co-culture times.

The limited cell survival time on PDMS villous scaffold can be explained by two reasons. Firstly, even though PDMS has relatively high gas permeability [5], the permeability of nutrients through PDMS, for example glucose, is limited, which makes it difficult for cells to uptake growth media from the basolateral side [17]. Secondly, PDMS itself lacks the capability of supporting cell attachment and proliferation. Once the collagen coated on the surface of PDMS villous scaffold is used up during the culture process, cells are likely to detach from the PDMS.

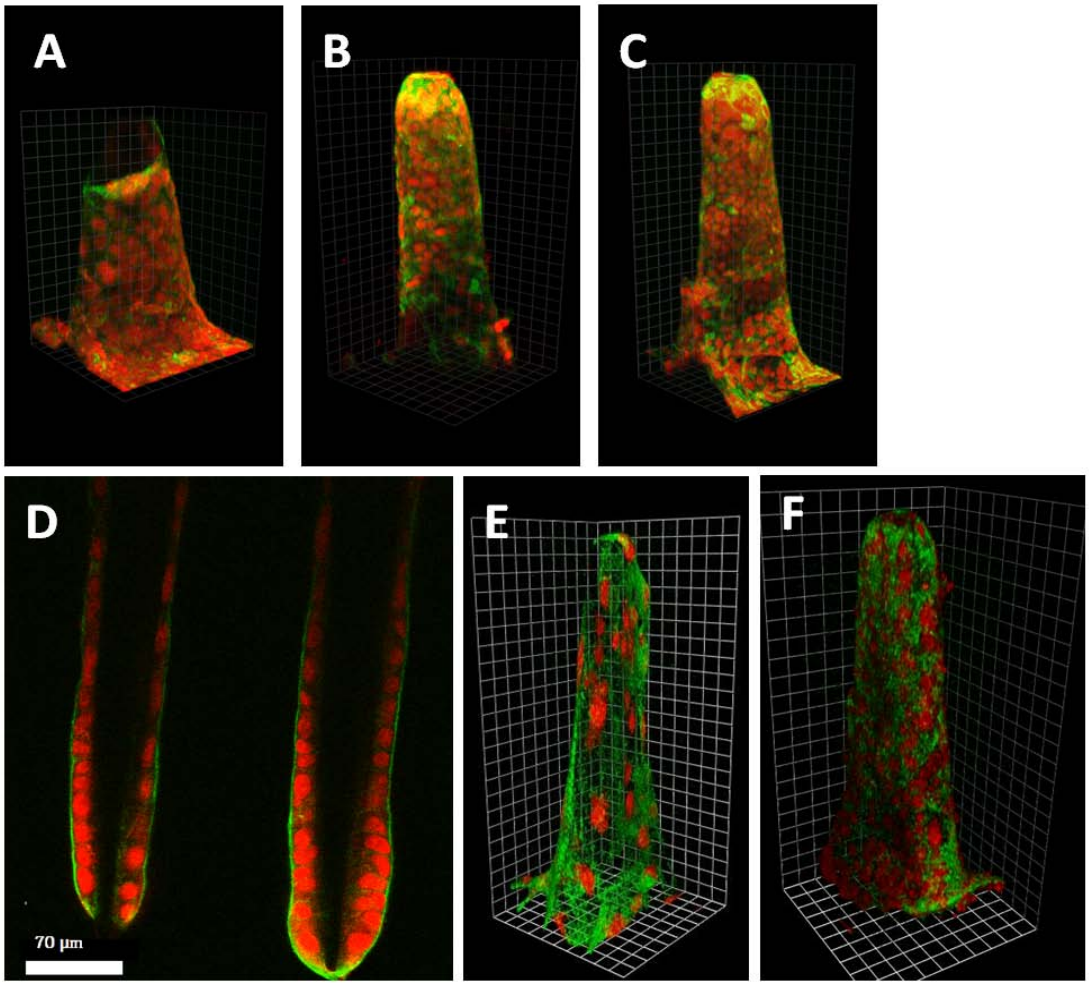

Figure 2.6 (A-D) Human carcinoma cells (Caco-2) were seeded on the PDMS scaffolds and allowed to grow to confluency (A: 4 days post seeding, B: 7 days, C: 12 days, D: longtitudinal sections at 7 days). (E) Human mesenchymal stem cells (hMSCs) on the PDMS scaffolds. (F) Co-culture of hMSC cells and IEC-6 Cdx2 HNF4-α cells on 3D scaffolds (4 days post IEC-6 seeding). Actin was stained green and nucleic acid was stained red. 1 unit = 22.1 µm.

Cell culture on collagen scaffold

Due to the problems encountered by using PDMS scaffold, a collagen hydrogel was chosen to overcome the cell growth and basolateral side feeding problems due to its "cell friendly" and porous characteristics. We seeded the cells onto the collagen scaffold and cultured for up to three weeks. As cells proliferated, they invaded and covered the collagen villi. The image of the collagen structure covered with cells is shown in Figure 2.7A. The overall morphology of the cell-covered collagen structure shows a striking similarity to the scanning electron microscope image of human jejunal villi, shown in Figure2.7B as a reference [20]. The x–y slice image of stained cells (Figure 2.7C) shows that the cells proliferated around the collagen scaffold, forming a uniform coverage.

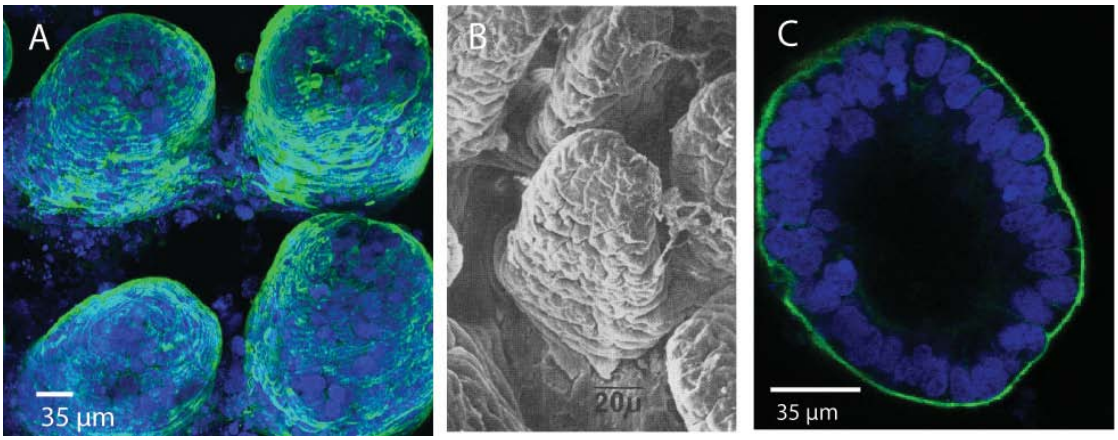

Figure 2.7 (A) Confocal microscope image of Caco-2 cells on collagen scaffold, after staining for actin (green) and nucleic acid (blue). (B) Scanning electron microscope image of human jejuna villi (reproduced with permission from BMJ group [20]). Confocal microscope image (x-y slice) of Caco-2 cells on the collagen scaffold, stained for actin (green) and nucleic acid (blue).

After cells completely covered the collagen surface, it was observed that the height of the collagen structure was reduced to about 250 μm, which is about half of the original size (Figure 2.8A). This change was not due to the instability of the collagen scaffold, as it remained intact while immersed in cell culture medium for three weeks (Figure 2.8B). The decrease in height was probably caused by several factors, including the tension from the cells attached to the collagen matrix, degradation of collagen during invasion of cells into the matrix, and formation of a cell multilayer at the bottom surface.

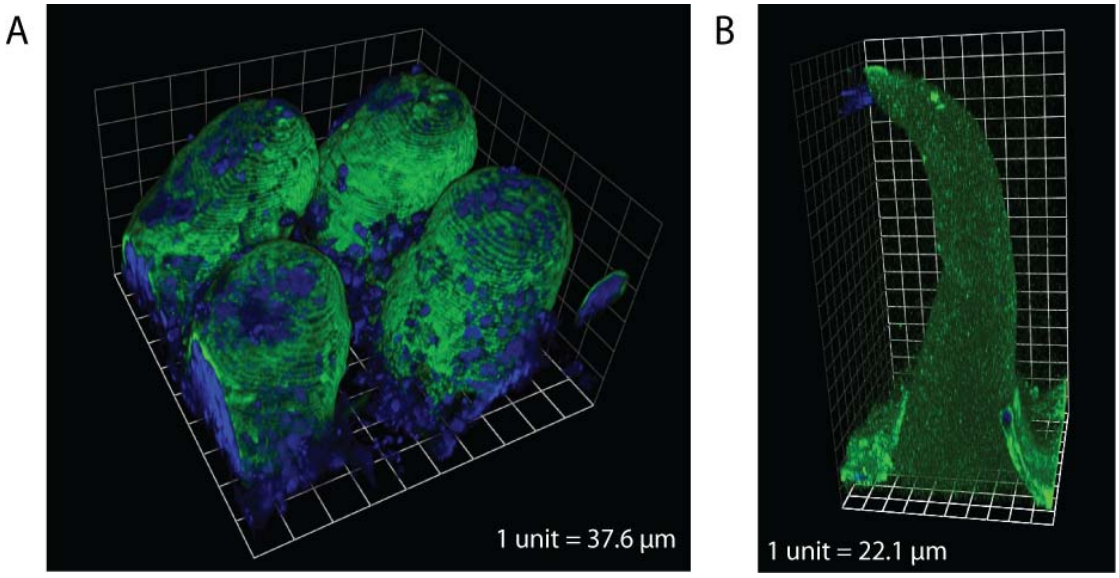

Figure 2.8 3D rendered image of collagen scaffold (A) covered with cells and (B) without cells

DISCUSSION

This study describes a method for creating a hydrogel scaffold mimicking the microscale 3D geometries of biological tissues. This method offers several advantages over currently existing methods for microfabrication of hydrogels. Using alginate as a sacrificial layer is particularly advantageous since the alginate dissolving process is physiologically mild, and therefore compatible with applications involving cells. Furthermore, this method is relatively simple and the whole process can be carried out easily on a common lab bench or a biosafety cabinet for sterility. It does not require expensive or complicated equipments such as a cleanroom, which is required by most of microfabrication methods. Finally, this method should be compatible with various hydrogels, not only collagen and PEG-DA used in this study, and with other complex shapes of biological tissues. Although using a hydrogel as a sacrificial layer has been demonstrated previously [8], this method mainly focused on fabrication of a two-dimensional microfluidic network. Our method is more versatile, as it allows fabrication of arbitrary 3D shapes.

Physiologically realistic 3D models of intestinal villi may greatly improve in vitro drug absorption studies, allowing for improved predictability when compared to conventional Caco-2 monolayers [2]. In this study, cells were grown on the surface of a fabricated hydrogel scaffold to mimic the intestinal villi epithelium. Culturing additional cells encapsulated in the hydrogel scaffold would make an even more physiologically realistic in vitro model. For example, we further plan to encapsulate vascular endothelial cells inside the collagen scaffold to mimic the vascular structure

of the intestine. Another approach is to integrate the fabricated hydrogel structure within a microfluidic device to explore using the 3D villi model as a tool for drug absorption studies. Integration with a two-layer microfluidic device will enable simulation of basolateral and apical flow of the intestine. Through analysis of the flow on both sides one can study the dynamics of drug absorption through the GI tract. Examining the biological activity of the Caco-2 cells cultured on the 3D scaffold, possibly co-cultured with other supporting cell types [19, 28] will reveal the effect of having physiologically correct 3D geometry on cell functions. We believe that this method will contribute significantly to several research disciplines, such as tissue engineering, pharmaceutical sciences, and cell biology.

ACKNOWLEDGEMENTS

This work was supported by Nanobiotechnology center (NBTC) at Cornell University, Army Corp of Engineers (CERL, W9132T-07), and The Hartwell Foundation. This work was also supported by Microscopy and Imaging Facility (MIF), Cornell Nanoscale Science and Technology Facility (CNF) at Cornell University. The authors thank Dr. Michael Campalongo for help with SEM images of the PDMS villi, Glenn Swan for fabricating the gasket, and Dr. Nakwon Choi and Dr. Abraham Stroock for helping the design of the gasket.

REFERENCES

1. Abbott A (2003) Cell culture: Biology's new dimension. Nature 424:870-872

2. Artursson P, Palm K, Luthman K (2001) Caco-2 monolayers in experimental and theoretical predictions of drug transport. Advanced Drug Delivery Reviews 46:27-43

3. Benton JA, Fairbanks BD, Anseth KS (2009) Characterization of valvular interstitial cell function in three dimensional matrix metalloproteinase degradable PEG hydrogels. Biomaterials 30:6593-6603

4. Bian W, Liau B, Badie N, Bursac N (2009) Mesoscopic hydrogel molding to control the 3D geometry of bioartificial muscle tissues. Nature protocols 4:1522-1534

5. Charati SG, Stern SA (1998) Diffusion of Gases in Silicone Polymers: Molecular Dynamics Simulations. Macromolecules 31:5529-5535

6. Choi NW, Cabodi M, Held B, Gleghorn JP, Bonassar LJ, Stroock AD (2007) Microfluidic scaffolds for tissue engineering. Nat Mater 6:908-915

7. Cushing MC, Anseth KS (2007) Materials science. Hydrogel cell cultures. Science 316:1133-1134

8. Golden AP, Tien J (2007) Fabrication of microfluidic hydrogels using molded gelatin as a sacrificial element. Lab on a Chip 7:720-725

9. Gough JE, Scotchford CA, Downes S (2002) Cytotoxicity of glutaraldehyde crosslinked collagen/poly(vinyl alcohol) films is by the mechanism of apoptosis. Journal of Biomedical Materials Research 61:121-130

10. Guillemot F, Souquet A, Catros S, Guillotin B, Lopez J, Faucon M, Pippenger B, Bareille R, Rémy M, Bellance S, Chabassier P, Fricain JC, Amédée J (2010) High-throughput laser printing of cells and biomaterials for tissue engineering. Acta Biomaterialia 6:2494-2500

11. Karuri NW, Liliensiek S, Teixeira AI, Abrams G, Campbell S, Nealey PF, Murphy CJ (2004) Biological length scale topography enhances cell-substratum adhesion of human corneal epithelial cells. Journal of Cell Science 117:3153-3164

12. Khademhosseini A, Langer R (2007) Microengineered hydrogels for tissue engineering. Biomaterials 28:5087-5092

13. Kim D-H, Lipke EA, Kim P, Cheong R, Thompson S, Delannoy M, Suh K-Y, Tung L, Levchenko A (2010) Nanoscale cues regulate the structure and function of macroscopic cardiac tissue constructs. Proceedings of the National Academy of Sciences 107:565-570

14. Klank H, Kutter JP, Geschke O (2002) CO2-laser micromachining and back-end processing for rapid production of PMMA-based microfluidic systems. Lab on a Chip 2:242-246

15. Koo LY, Irvine DJ, Mayes AM, Lauffenburger DA, Griffith LG (2002) Co-regulation of cell adhesion by nanoscale RGD organization and mechanical stimulus. Journal of Cell Science 115:1423-1433

16. Lee W, Lee V, Polio S, Keegan P, Lee J-H, Fischer K, Park J-K, Yoo S-S (2010) On-demand three-dimensional freeform fabrication of multi-layered hydrogel scaffold with fluidic channels. Biotechnology and Bioengineering 105:1178-1186

17. Liu L, Sheardown H (2005) Glucose permeable poly (dimethyl siloxane) poly (N-isopropyl acrylamide) interpenetrating networks as ophthalmic biomaterials. Biomaterials 26:233-244

18. Lussier CR, Babeu J-P, Auclair BA, Perreault N, Boudreau F (2008) Hepatocyte nuclear factor-4α promotes differentiation of intestinal epithelial cells in a

coculture system. American Journal of Physiology - Gastrointestinal and Liver Physiology 294:G418-G428

19. Mahler GJ, Shuler ML, Glahn RP (2009) Characterization of Caco-2 and HT29-MTX cocultures in an in vitro digestion/cell culture model used to predict iron bioavailability. The Journal of Nutritional Biochemistry 20:494-502

20. Marsh MN, Swift JA (1969) A study of the small intestinal mucosa using the scanning electron microscope. Gut 10:940-949

21. Nguyen KT, West JL (2002) Photopolymerizable hydrogels for tissue engineering applications. Biomaterials 23:4307-4314

22. Park H, Cannizzaro C, Vunjak-Novakovic G, Langer R, Vacanti CA, Farokhzad OC (2007) Nanofabrication and microfabrication of functional materials for tissue engineering. Tissue engineering 13:1867-1877

23. Peppas NA, Huang Y, Torres-Lugo M, Ward JH, Zhang J (2000) PHYSICOCHEMICAL FOUNDATIONS AND STRUCTURAL DESIGN OF HYDROGELS IN MEDICINE AND BIOLOGY. Annual Review of Biomedical Engineering 2:9-29

24. Suri S, Schmidt CE (2010) Cell-laden hydrogel constructs of hyaluronic acid, collagen, and laminin for neural tissue engineering. Tissue engineering. Part A 16:1703-1716

25. Talei Franzesi G, Ni B, Ling Y, Khademhosseini A (2006) A Controlled-Release Strategy for the Generation of Cross-Linked Hydrogel Microstructures. Journal of the American Chemical Society 128:15064-15065

26. Tortora GJ, Grabowski SR (1993) Principles of anatomy and physiology. HarperCollinsCollege, New York

27. Tsang VL, Bhatia SN (2007) Fabrication of three-dimensional tissues. Advances in biochemical engineering/biotechnology 103:189-205

28. Walter E, Janich S, Roessler BJ, Hilfinger JM, Amidon GL (1996) HT29-MTX/Caco-2 cocultures as an in vitro model for the intestinal epithelium: In vitro–in vivo correlation with permeability data from rats and humans. Journal of Pharmaceutical Sciences 85:1070-1076

29. Yen TH, Wright NA (2006) The gastrointestinal tract stem cell niche. Stem cell reviews 2:203-212

CHAPTER THREE:

IN VITRO 3D HUMAN SMALL INTESTINAL VILLOUS MODEL FOR DRUG PERMEABILITY DETERMINATION

Yu J [a], Peng S [a], Luo D [a], March JC [*a] (2012) In vitro 3D human small intestinal villous model for drug permeability determination. Biotechnology and Bioengineering 109:2173-2178 - Reproduced by permission of John Wiley & Sons

[a] Biological and Environmental Engineering, Cornell University, USA.

ABSTRACT

We present a novel method for testing drug permeability that features human cells cultured on collagen based hydrogel scaffolds made to accurately replicate the shape and size of human small intestinal villi. We compared villous scaffolds to more conventional 2D cultures in paracellular drug absorption and cell growth experiments. Our results suggest that 3D villous platforms facilitate cellular differentiation and absorption more similar to mammalian intestines than can be achieved using conventional culture. To the best of our knowledge, this is the first accurate 3D villus model offering a well-controlled microenvironment that has strong physiological relevance to the in vivo system.

INTRODUCTION

Over two decades ago, a human intestinal in vitro model was developed by culturing a human colonic carcinoma cell line (Caco-2) on microporous filters [9]. When forming a monolayer under normal culture conditions, Caco-2 cells spontaneously differentiate into columnar and polarized cells that have similar resistance and permeability as small intestinal enterocytes [9, 16]. Since its development, this 2D model has being widely used for permeability testing of new drug candidates as well as investigating functionality of different intestinal transporters [1, 3, 4, 8]. While the 2D model has been proven accurate for transcellularly-transported drugs, the correlation between the 2D model and the human intestine for carrier-mediated and paracellularly-transported drugs is poor [2, 4, 6, 13]. For drugs transported via the carrier-mediated pathway, research has demonstrated that poor correlations are cell line-related and that the

Caco-2 cell line can have significant differences in transport-related gene expression levels when compared to the human intestine [19]. For drugs absorbed via the paracellular pathway, poor correlations are mostly attributed to two factors: (1) the difference in tight junction formation between Caco-2 cell monolayers and human small intestine epithelia and (2) the lack of intestinal villi in 2D models[4]. Intestinal cell lines with leakier tight junctions have been used to improve the correlation to human intestines of paracellularly-absorbed drugs [7, 21]. However, recently it has been shown that Caco-2 cell monolayers have similar paracellular pore size distributions as human intestinal epithelia, even though, on average, the porosity of Caco-2 monolayers is smaller [14]. Taken together, these findings suggest that there may be an as yet undetermined role for the 3D microenvironment in controlling epithelial barrier function.

Making use of newly developed microfabrication techniques and biocompatible materials, new in vitro models of the small intestinal microenvironment have been reported. For example, a microfluidic device fitted with a cell culture analog was recently used to mimic the human gastrointestinal tract on a microscopic scale [15]. In other work intestinal crypt-like topography was fabricated into a cell culture system, although the size of the crypt structures was significantly smaller than actual crypts [23]. We recently reported fabricating hydrogel structures with high aspect ratio and curvature at the micro-scale using a combination of laser fabrication and sacrificial molding [20]. However, despite recent advances no one has been able to demonstrate the relevance of the 3D environment to epithelial barrier function.

To begin to answer this question, we present here a new method for performing a drug permeability test that makes use of 3D biomimetic scaffolds to impart physiological relevance to an in vitro model. Intestinal villi scaffolds were fabricated using, first a CO2 laser to form an 8 by 8 mm2 villi array mold on polymethylmethacrylate (PMMA) sheet. The density of the villi mold was intended to simulate actual villi spacing at 25 villi/mm^2 and the depth of a single villous mold was approximately 565 μm, which is in the physiological range of human small intestinal villi [22]. A collagen scaffold was made from the mold using previously described techniques [20]. A well plate insert was designed to integrate the hydrogel scaffold into a standard 6-well culture plate. The goal of this study was to determine the role of the 3D microenvironment in establishing barrier function and to improve existing in vitro intestinal models by incorporating widely-available biomaterials.

MATERIALS AND METHODS

Laser fabrication

Polymethylmethacrylate PMMA sheet (Ithaca Plastic, Ithaca, NY) was used as a template. A CO_2 laser system VersaLaser VLS3.50 (Versatech, USA) with controlling software Corel Draw X5(Corel, Mountain View, CA) was used, which gave a much higher etching capability than the UV laser used in previous work [20]. An 8 mm by 8 mm oval array with 25 ovals per square millimeter density was drawn using the software package. The long axis of a single oval is 100 μm, the short axis is 60 μm. To prevent over melting of the PMMA surface by the laser, the etch model was set as

VECT with 10% laser power, 100% laser speed and 1000 Pulses Per Inch (PPI). The PMMA mold was etched with different copy times in order to achieve an ideal depth. Hole depth was measured by an Olympus BX61 upright microscope system (Olympus Imaging America, Center Valley, PA) using the Z-series function. The final PMMA mold was made under this setting with 4 distinct etch times.

Fabrication of collagen villi hydrogel

The collagen villi hydrogel was fabricated using previously reported methods [20]. Briefly, a Polydimethylsiloxane (PDMS) villi structure mold was made from a PMMA mold. The PDMS villi mold was glued on an aluminum gasket to make an alginate reverse mold, which was cured with a 60 mM calcium chloride solution. The collagen hydrogel scaffold was made by 5 mg/ml type I collagen (Sigma, St. Louis, MO) from the alginate reverse mold. After curing collagen at 37 °C with 0.3% glutaraldehyde overnight, the alginate mold was dissolved in a 60 mM EDTA solution. The collagen hydrogel scaffold was washed with PBS buffer for three days before use. The 2D collagen was fabricated using the same method but without villi structure in the PMMA mold.

Cell culture

The human colon carcinoma cell line Caco-2 (passage number 16-25, ATCC, Manassas, VA) was used in this study. Caco-2 cells were maintained in Dulbecco's Modified Eagle's Media (Mediatech, Manassas, VA), with 10% FBS (Invitrogen,

Carlsbad, CA) and 1X anti-biotic anti-mycotic (Invitrogen, Carlsbad, CA). Caco-2 cells were maintained in a 37 °C incubator with 5% CO2 gas.

Design of well-plate insert

Our well plate insert design was based on existing inserts so that they can be directly added to commercially available plates (Figure 3.1, Figure3.2). In this design, a hydrogel scaffold either with or without (as a 2D control) synthetic villi is placed in the bottom of the supporting structure and sealed by a size 10 O-ring (0.289 cm2 sealing area) (Figure 3.1A). Screws were used to tighten the top gasket into the supporting insert, which allows the operator to apply the correct amount of pressure to the upper insert to make a seal. A dye test was performed to insure that there was no leaking around the hydrogel (Figure 3.1B) and that the integrity of hydrogel was still intact after being sealed (Figure 3.1C). The whole insert is compatible with ordinary 6 well culture plates (Figure 3.1D). The insert kit was autoclaved and assembled with the collagen hydrogel scaffold using sterile tweezers. Assembled kits were placed into six-well plates (one well at a time) using sterile tweezers.

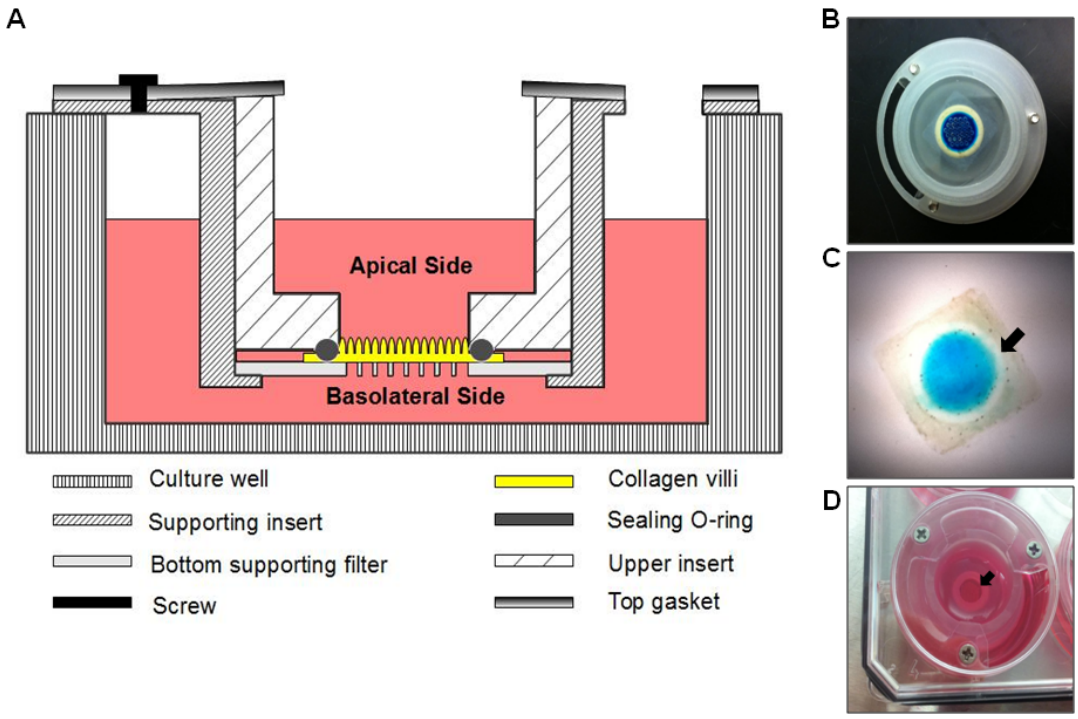

Figure 3.1. Overview of the insert kit (A) Schematic of the insert design (B) Dye test result of the insert, an O-ring was used to completely seal the villous insert within the culture well and prevent short-circuiting around the test area. (C) When the scaffolding was removed from the culture well, the scaffolding layer did not rupture and the dye remained within the villous test area. (Arrow points to the O-ring sealing area) (D) An image of a modified well inserted in a 6 well plate. (Arrow points to the area actually covered by synthetic villi)

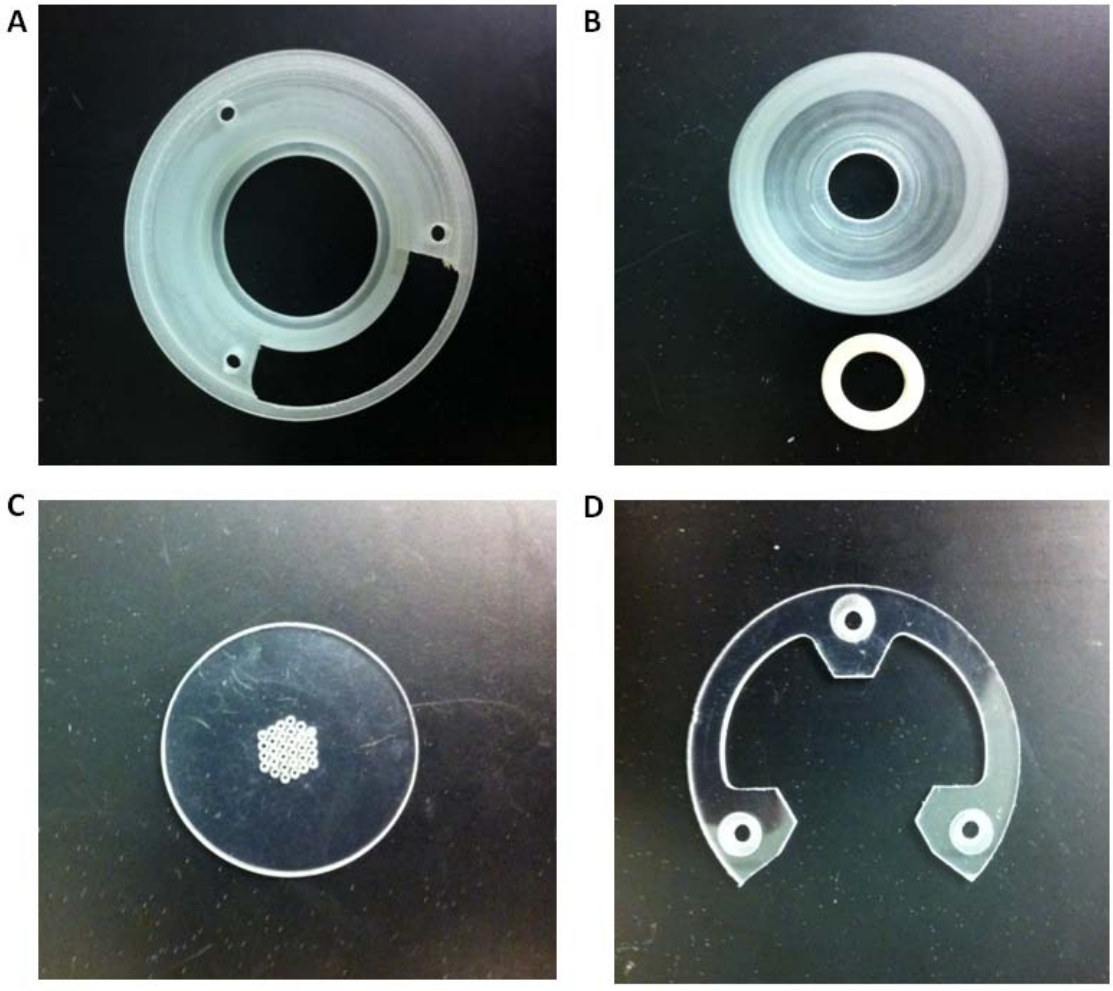

Figure 3.2 Pictures of insert kit. (A) Supporting insert (B) Upper insert and O-ring (C) Bottom supporting filter (D) Top gasket

Dye test

Collagen hydrogel scaffolds were assembled inside insert kits. NEON blue food dye solution (McCormick & Co, Hunt Valley, MD) was added to apical side in order to observe its diffusion to the basolateral side. After visually checking for leaks, the collagen hydrogel scaffolds were detached from the insert kits and inspected for integrity.

Trans Epithelial Electric Resistance measurement

Trans Epithelial Electric Resistance (TEER) was measured with EVOM2 Epithelial Voltohmmeter with STX3 electrode (World Precision Instruments, Sarasota, FL). Electrodes were places on the apical and basolateral sides of the insert kits in order to measure TEER across the 2D and 3D cultures. Standard 0.4 µm pore size cell culture inserts (Corning Incorporated, Corning, NY) were used for measuring Caco-2 TEER under conventional conditions.

Drug permeability test

Drug permeability testing was conducted following a standard protocol [11] with the following adjustments. After being sealed into an insert kit, collagen hydrogel scaffolds were coated with 200 µg/mL Laminin (Sigma -Aldrich, St. Louis, MO) in 37°C for 2h. After being washed by PBS for three times, scaffolds were seeded with 20 µL 1×10^6 cells/ml Caco-2 cells and incubated (37°C with 5% CO_2 gas) for 1h to allow cell attachment. After checking cell attachment, 1.5 mL culture media was added into the apical side of the insert kit and 2.6 mL culture media was added to basolateral side. Media was exchanged 1 day after seeding and every 2 days during the experiment. Hank's balanced salt solution (Sigma-Aldrich, St. Louis, MO) was buffered with 25 mM HEPES and 0.35 g/L $NaHCO_3$ and adjusted to pH 7.4 to be used as HESS buffer in this experiment. The permeability test was conducted after 14 days culture because longer culture times resulted in shorter villous heights and multiple cell layers penetrating the villus scaffold [20]. Prior to the permeability test, media was aspirated from both apical and basolateral sides and 37°C pre-warmed HESS was

added apically and basolaterally. The TEER value and cell monolayer morphology were checked to make sure that only scaffolds with no monolayer disintegration were used. The plates were incubated (37°C with 5% CO_2 gas) on a 500 rpm orbital shaker (MTS 2/4 digital shaker, IKA@ Works, Wilmington, NC) for 15 min then HESS buffer was removed and the inserts were transferred to new six-well plates. Three hundred microliters 37°C Antipyrine (0.1 mM in HESS, pH 7.4) or Atenolol (2.0 mM in HESS, pH 7.4) solution was added to apical side of the inserts and 100 µL was immediately taken for measuring C_0. Six milliliters 37°C HESS solution was added to the basolateral side to eliminate the hydrostatic pressure difference between the apical and basolateral chambers. The six-well plates were incubated (37°C with 5% CO_2 gas) on a 500 rpm orbital shaker to minimize the impact of the unstirred water layer. At specific time intervals, a 3 mL sample was collected from the basolateral side and replaced by 3 mL 37°C HESS solution. For each permeability test at least, three samples were taken within a 2 h period. A 100 µL sample was taken from the apical side of the insert for measuring C_f at the last sample point. After completion of the permeability test, TEER was measured to insure that monolayer integrity was intact. The hydrogel scaffolds were then detached from the insert kit and fixed in a 4% formaldehyde solution for confocal scanning. The permeability coefficient was calculated based on a non-sink condition and only mass balances greater than 90% were used. Details of permeability coefficient calculation can be found in more detail elsewhere [11]. Briefly, the permeability coefficient P_{app} (cm/s) was calculated according to the follow equation:

$$P\text{app}=(\mathrm{d}Q/\mathrm{d}t)\ (1/(AC_0))$$

where (dQ/dt) is the rate of appearance of drug on the receiving side (μmol/s), A is the cross-sectional area of the barrier (cm^2), and C_0 is the initial drug concentration on the donor side (μmol). In this study, A is the O-ring sealing area, which is 0.289cm^2 for both 2D and 3D collagen. For conventional insert data, permeability tests were conducted after 14 or 21 days culture using 12-well plate inserts. Each permeability measurement was replicated 4 times. Student's *t*-tests were used to determine statistically significant differences.

High performance liquid chromatography analysis

High performance liquid chromatography (HPLC) was used to measure the drug concentrations in the permeability tests through a reverse-phase C18 column (250 × 4.6 mm^2, 5 μm, Phenomenex, Torrance, CA) equipped with a photodiode array detector (210 nm-400 nm, Waters Corporation, Milford, MA). Elution A was aqueous 0.1% trifluoroacetic acid (TFA) and elution B was acetonitrile in 0.1% TFA. A gradient of 5%-30% B at a flow rate of 1.0 ml/min was used, and the column was maintained at 25 °C. The absorbance was measured at 225 nm for Atenolol, and 254 nm for Antipyrine, respectively

.

Immunofluorescence

Mouse small intestine paraffin sections were obtained from C57BL/6J (B6) male mice at 18 weeks age. Adult Human small intestine paraffin sections were obtained from Dr. David J. Hackam Lab at Children's Hospital of Pittsburgh of UPMC as a gift. Paraffin sections were washed 3 times in xylene solution for 5 min each followed by

washes with 100%, 90% and 70% ethanol solutions for 5 min each respectively. Before the antigen unmasking, paraffin sections were washed in DI water twice. For antigen unmasking, paraffin sections were submerged in 0.01M citrate acid buffer pH 6.0 in a sealed container and boiled in a steam cooker (Stanley Black & Decker, New Britain, CT) for 40 min. After three washes in DI water, paraffin sections were blocked by blocking buffer which contained 1X PBS buffer with 5% normal donkey serum and 0.3% Triton X-100 in room temperature for 60 min. Then paraffin sections were covered by 200 µl 1:50 diluted Alkaline Phosphatase antibody solution (4 µg/ml final concentration, catalog number L19, Santa Cruz Biotechnology, Santa Cruz, CA) and incubated at 4°C overnight. After being washed by PBS for three times, paraffin sections were incubated with 200 µl 1: 1000 diluted Alexa Fluor 488 donkey anti-goat secondary antibody solution (2 µg/ml final concentration, Invitrogen, Carlsbad, CA) for 60 min in room temperature. Before imaging, paraffin sections were washed by PBS three times and stained by TO-PRO-3 (Invitrogen, Carlsbad, CA) for nucleic acid staining.

Imaging and analysis

Light microscopy was performed on a Leica DM IL LED invented microscope (Leica Microsystems, Buffalo Grove, IL). For confocal scanning, cell samples were stained by Alexa Fluor 488 phalloidin (Invitrogen, Carlsbad, CA) and TO-PRO-3 for actin and nucleic acid staining, respectively. Samples were scanned using a Leica SP2 confocal microscope (Leica Microsystems, Buffalo Grove, IL) with Z-series capability. 3D rendering images and section pictures were assembled with Volocity

5.0 software (Perkin Elmer, Waltham, MA). Image analysis, cell density counting and villous parameter measurement were conducted with ImageJ software (NIH, Bethesda, MD).

RESULTS

Fabrication of PMMA mold using CO_2 laser

A CO_2 laser was used to fabricate PMMA mold. When compared to the UV laser used previously [20], the CO_2 laser not only has relatively lower cost but also can provide greater control over etching. The relationship between etch time and hole dept was determined (Figure 3.3) and each PMMA mold was etched 4 times to obtain an approximately 565 μm hole depth.

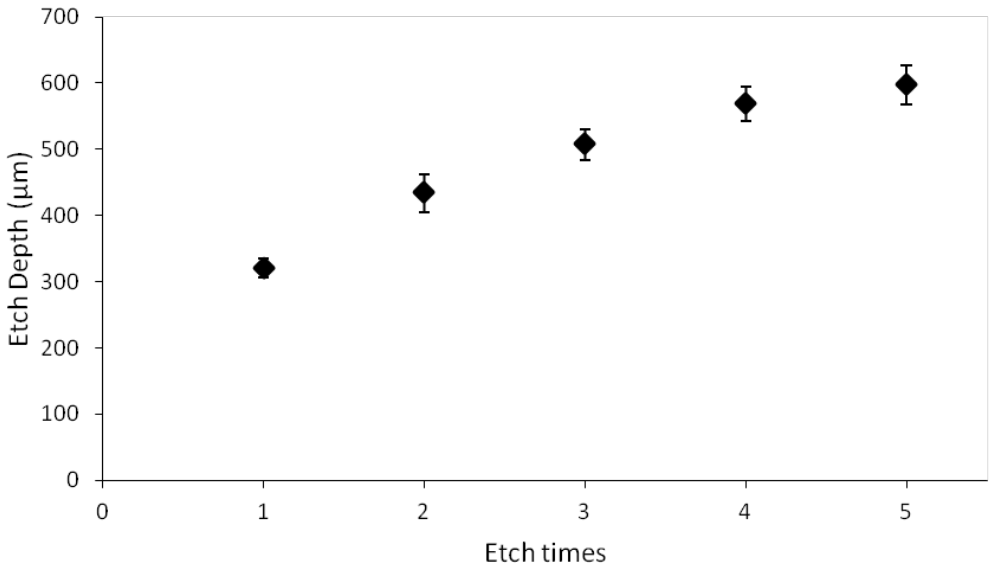

Figure 3.3 Relation between etch time and hole depth. The laser was running under 10% laser power, 100% laser speed and 1000 Pulses per Inch (PPI).

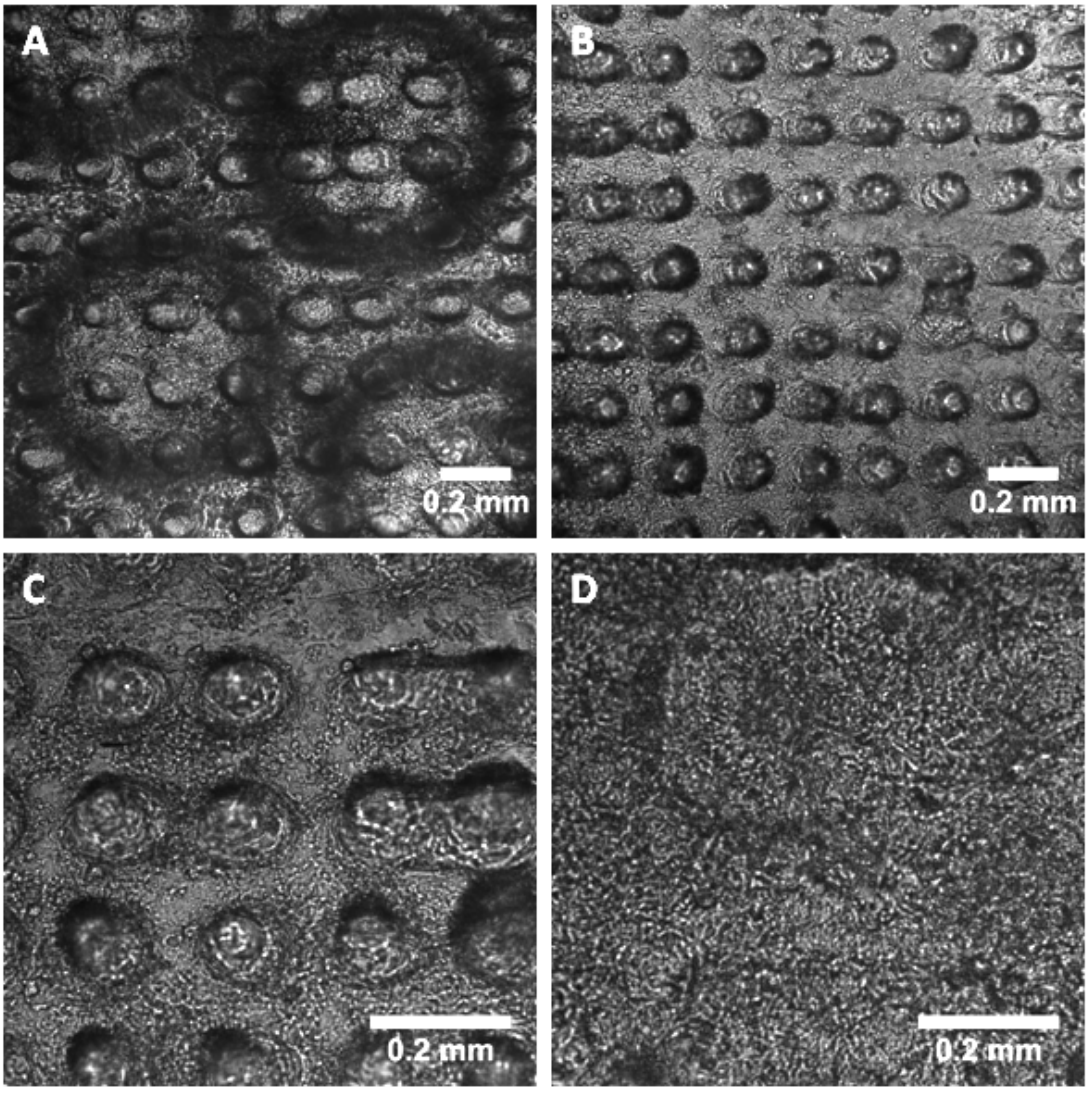

Figure 3.4 (A) 10x magnification picture of 3D scaffolds covered with 14 days cultured Caco-2 cell monolayer sealed in a well insert before a permeability test. The larger black rings are holes on the bottom supporting filter. (B) 10x magnification picture of a Caco-2 monolayer growing on 3D villous scaffolds after permeability test. (C) 20x magnification picture of a Caco-2 monolayer growing on 3D villous scaffolds after permeability test (D) 20x magnification picture of a Caco-2 monolayer on 2D collagen after a permeability test

Cell monolayer integrity before and after the permeability test

The insert design allows for observation of cell morphology on hydrogel scaffolds using ordinary 10x lenses in an inverted microscope (Figure 3.4A). After the permeability test, hydrogel scaffolds can be detached from the well insert and examined under higher magnification (Figure 3.4C, Figure 3.4D). Caco-2 cell monolayer integrity was inspected before and after each permeability test. In all cases, cell monolayer integrity was found intact (Figure 3.4).

Trans epithelial electric resistance (TEER) of cell monolayers

Although close inspection found no monolayer disintegration, TEER of Caco-2 monolayers grown on both the 2D and 3D collagen scaffolds was lower than that of Caco-2 monolayers grown on plastic inserts. TEER of Caco-2 monolayers grown on 3D collagen scaffolds was identical to that of perfused rat ileum [5], as well as human intestinal epithelia which was reported having TEER values ranging from 20 $\Omega \cdot cm^2$ in the jejunum to 100 $\Omega \cdot cm^2$ in the large intestine [10].

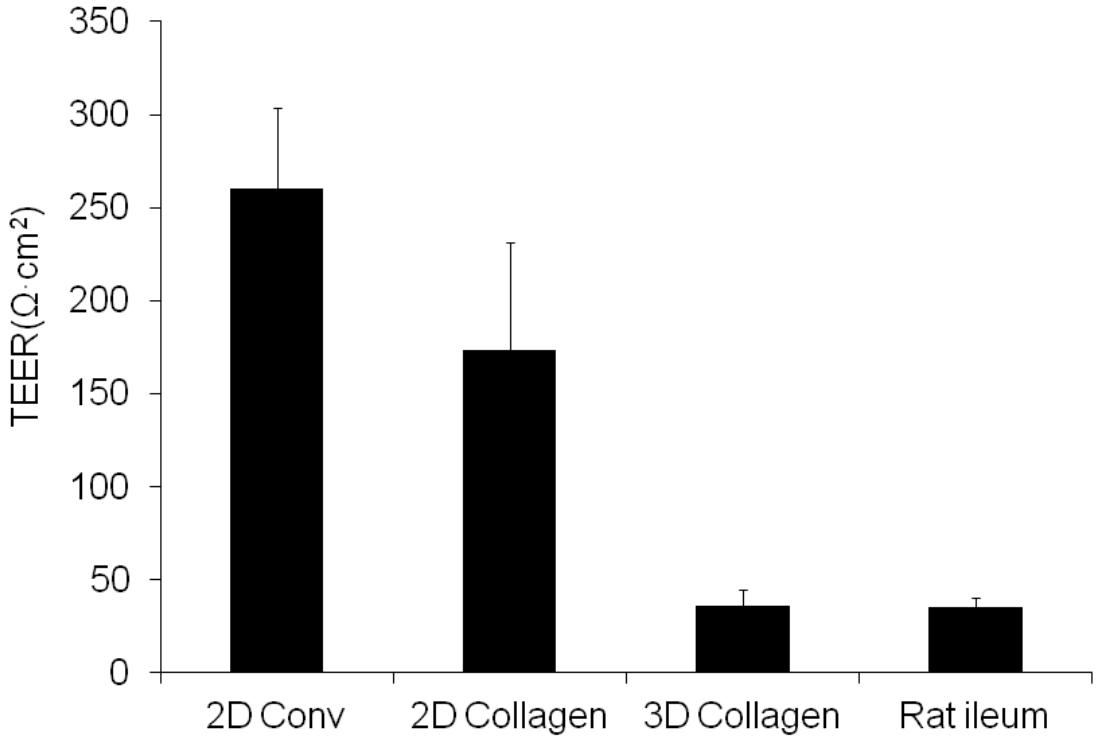

Figure 3.5 TEER of conventional Corning 0.4 µm polycarbonate cell culture insert with 14 days cultured Caco-2 cells (2D Conv), 2D collagen scaffolds with 14-day Caco-2 cell cultures (2D Collagen), 3D collagen scaffolds with 14-day Caco-2 cell cultures (3D Collagen) and rat ileum [5].

Comparing permeability coefficients of collagen scaffolds to conventional inserts

To test drug permeability, two drugs representing different absorption properties were selected: Antipyrine (hydrophobic, rapidly and completely absorbed drug) and Antenolol (hydrophilic, slowly and incompletely absorbed drug) [13]. For Antipyrine, the collagen hydrogel used was found to be the most significant transport barrier (Figure 3.6A), which suggests that collagen may not be suitable for rapid drug permeability testing. For Antenolol, scaffolds without cells had faster permeability

coefficients than the scaffolds with cells, hence the scaffolding was not considered a limiting factor (Figure 3.6B).

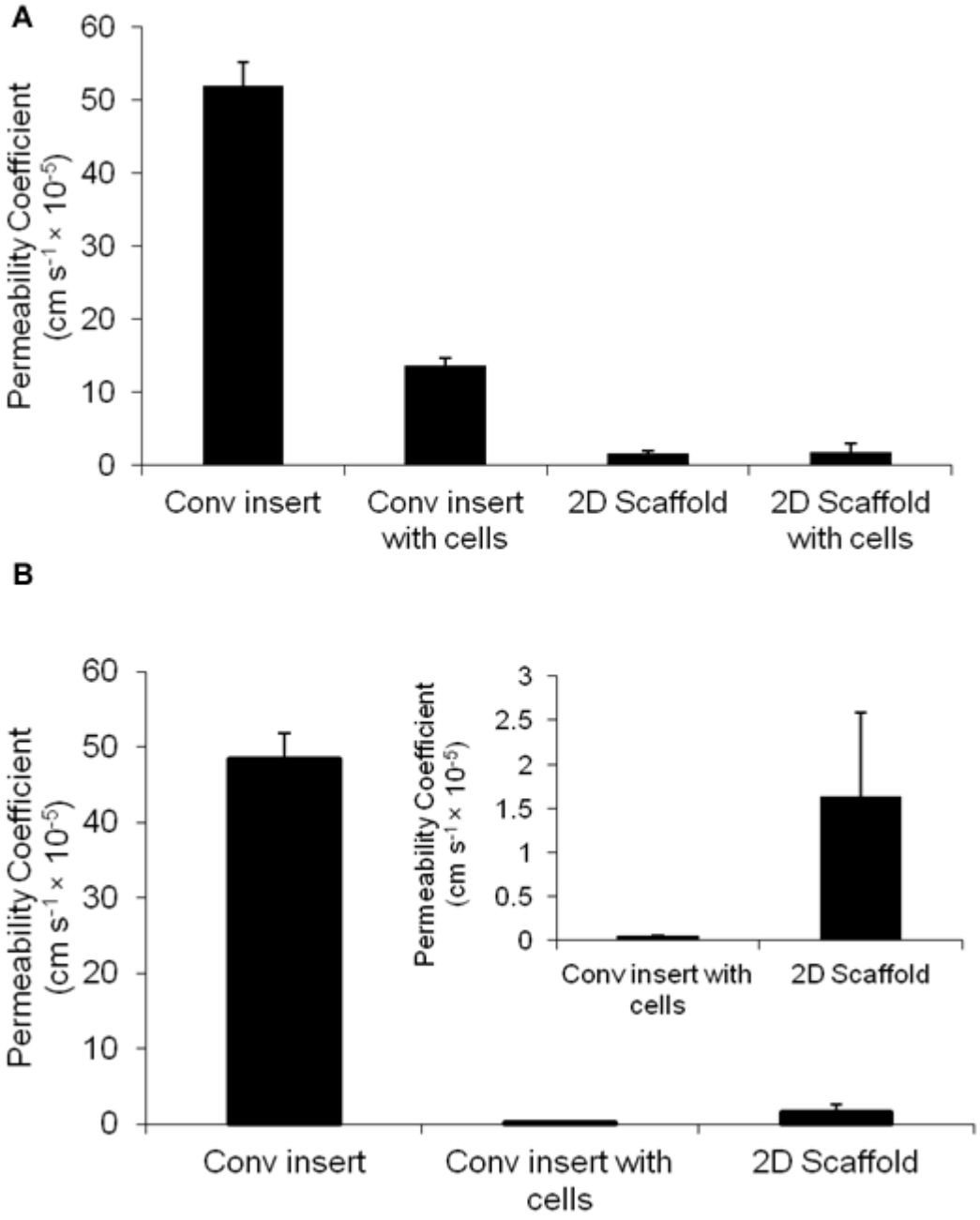

Figure 3.6 Comparing Permeability Coefficient of collagen scaffold to conventional insert. (A) Permeability coefficient of Antipyrine on Corning 0.4 µm polycarbonate

cell culture insert (Conv insert), insert with Caco-2 monolayer cultured 21 days (Conv insert with cells), 2D collagen scaffold (2D Scaffold) and 2D collagen scaffold with Caco-2 cells (2D Scaffold with cells) (B) Permeability coefficient of Atenolol on Corning 0.4 μm polycarbonate cell culture insert (Conv insert), insert with Caco-2 monolayer cultured 21 days(Conv insert with cells) and 2D collagen scaffold (2D Scaffold). Inset of Conv insert with cells and 2D Scaffold intended to more clearly show the difference.

The permeability coefficient of Caco-2 monolayers grown on 2D collagen scaffolds was not significantly different from the permeability coefficient of Caco-2 monolayers grown on conventional well inserts. Both of these values were at least 23 times lower than that of perfused human intestines (Figure 3.7) [12]. The permeability coefficient of Caco-2 monolayers grown on 3D collagen villi scaffolds was 13 times higher than that of Caco-2 monolayers grown on 2D collagen scaffolds and approximately more than half of the average value from perfused human intestines (Figure 3.7).

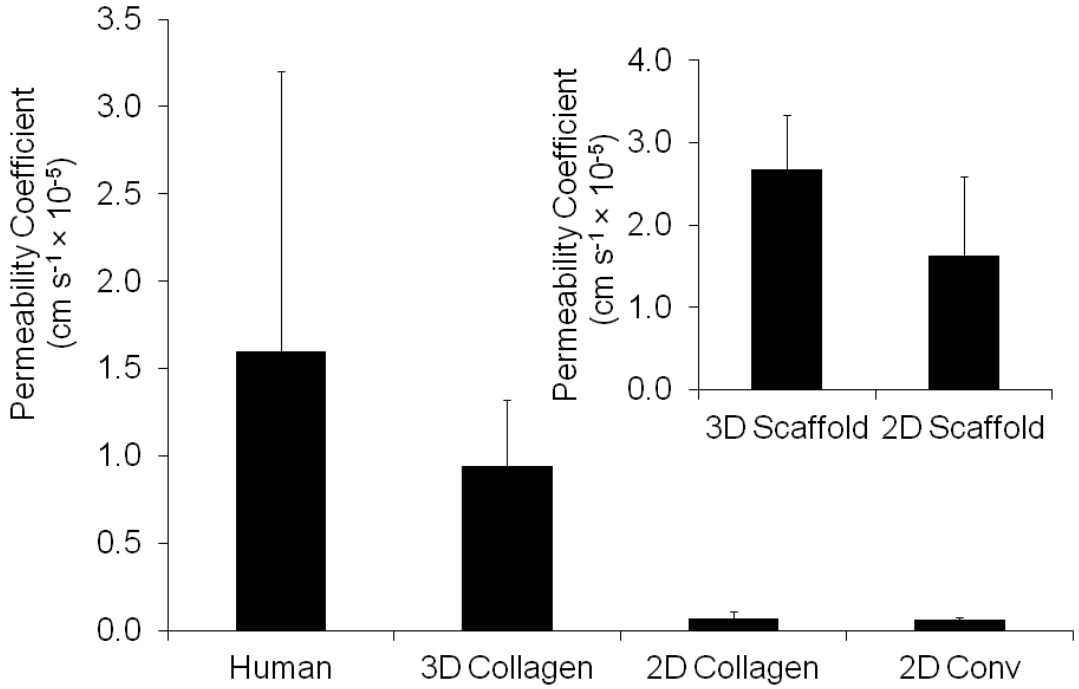

Figure 3.7 Permeability coefficients of Atenolol for perfused human intestine[12], 3D collagen scaffolds with 14-day Caco-2 cell cultures (3D Collagen), 2D collagen scaffolds with 14-day Caco-2 cell cultures (2D Collagen) and 2D Corning 0.4 µm polycarbonate cell culture insert with 14 days cultured Caco-2 cells (2D Conv). Inset is the permeability coefficients for just the 3D and 2D collagen inserts without cells (3D Scaffolds and 2D Scaffolds, respectively, 2D Scaffold is the same data used in Figure 3.6B).

Confocal microscopy scanning of cell morphology on 3D collagen scaffolds

Immediately following drug permeability testing, the collagen scaffolds with Caco-2 monolayers were detached from modified well inserts and scanned by confocal microscopy. Confocal scanning demonstrated that on 2D collagen scaffolds a polarized cell monolayer formed (Figure 3.8G). On 3D collagen scaffolds cells tended

to degrade the structures over time, resulting in heights of 330 µm on average by the end of the experiment (Figure 3.8A and B) [20]. Cell differentiation on 3D scaffolds varied along the villous length (in the X-Y orientation): cells were more polarized and columnar at the top and less differentiated near the villous base (Figure 3.8C, D, E, and F).

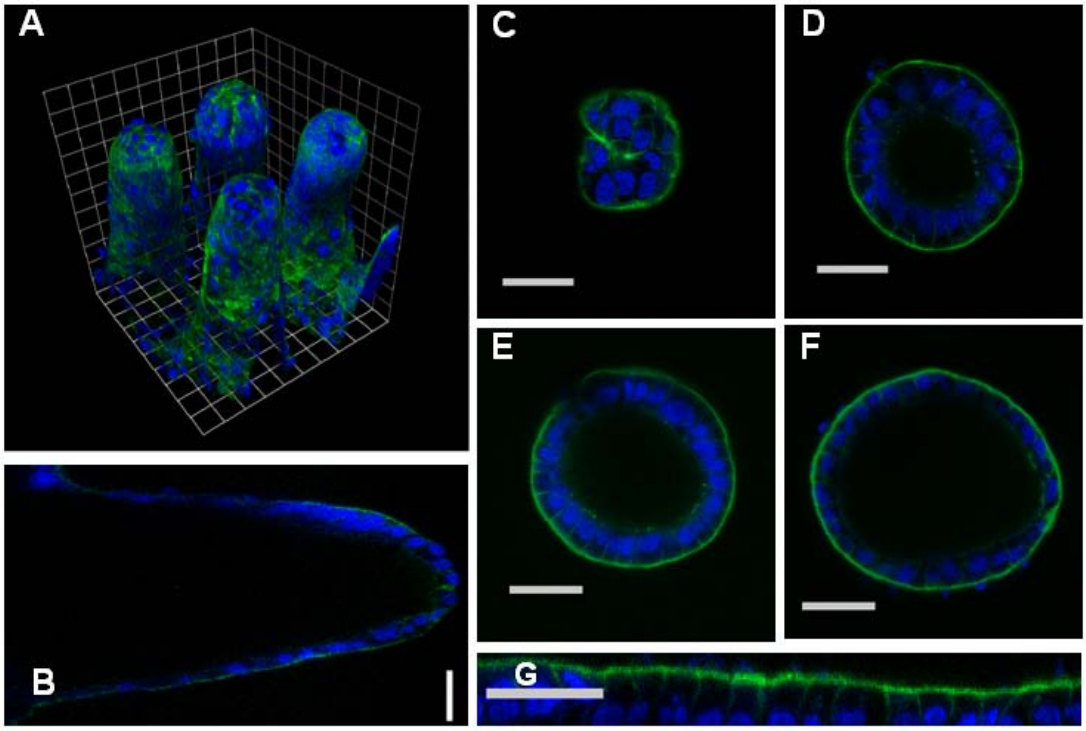

Figure 3.8 Confocal scanning pictures, cells are stained green (actin) and blue (nucleic acid). (A) 3D villi with Caco-2 cells after 3D rendering (1 unit=37.6µm) (B) X-Z section picture of single villous (C,D,E,F) Confocal X-Y section picture of single villous from top to bottom (G) X-Z section of a Caco-2 monolayer on 2D collagen. The scale bars in B, C, D, E, F and G are 43µm.

Cell density counts indicated that there was a slightly higher density of cells near the top of the villi than at the bottom (Figure 3.9). The actually surface area of 3D collagen villi was estimated. Size parameters of villi (average values) were estimated from confocal scans. The heights were 330 μm on average. The top and basal areas were treated as circles with 32.5 μm radii and 90 μm radii, respectively (Figure 3.10). The sealing area was measured as 0.289cm^2 and villi density was 25 villi per mm^2. The actually surface area of 3D collagen was 1.06cm^2, which was about 3.7 times higher than the surface area of the 2D scaffold (0.289cm^2).

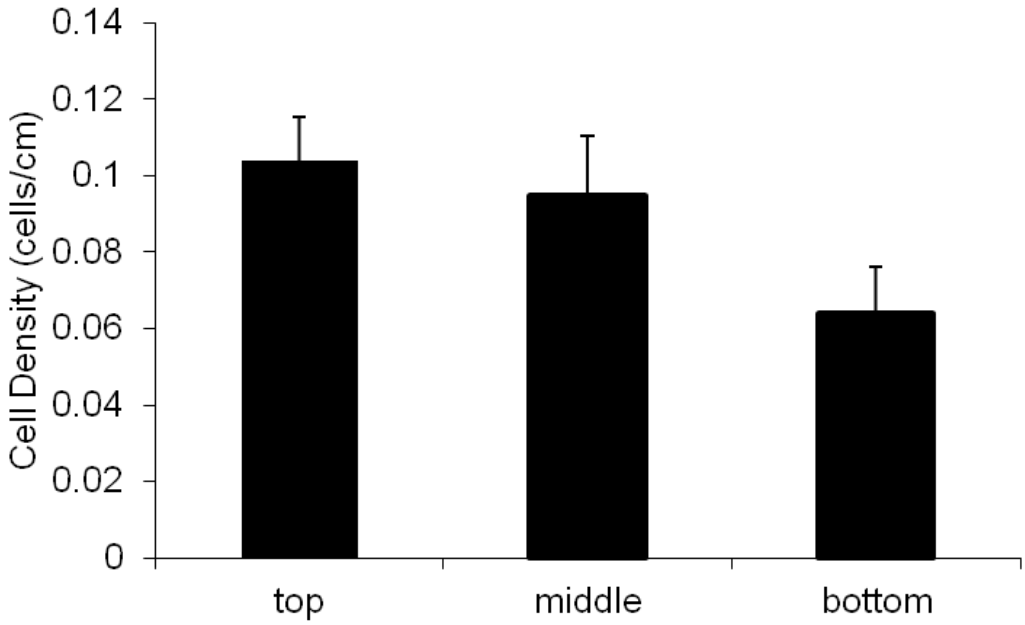

Figure 3.9 Cell density in X-Y section of a 3D collagen villus. Top, middle and bottom are related to the Z position of a single villus. Top sections were counted at approximately 200-300 μm from the base. Middle sections are approximately 100-200 μm from the base. Bottom sections are approximately 50-100 μm from the base.

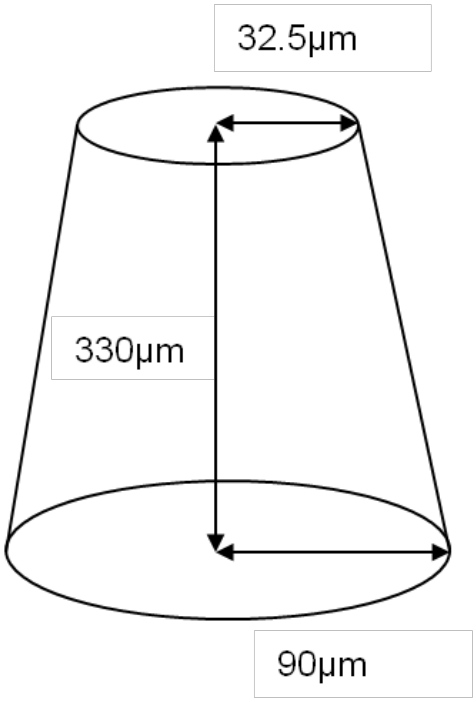

Figure 3.10 3D collagen villi surface area estimation

Adult mouse and human small intestine paraffin sections were used to investigate in vivo small intestinal epithelial differentiation (Figure 3.11). Alkaline Phosphatase, a brush border digestive enzyme which is frequently used as an enterocyte differentiation marker, was chosen as the target for immunofluorescence. In the mouse section, a uniform Alkaline Phosphatase immunofluorescence intensity was observed along the crypt-villus axis (Figure 3.11A). In contrast, in the human section, Alkaline Phosphatase immunofluorescence intensity increased along the crypt-villus axis (Figure 3.11B).

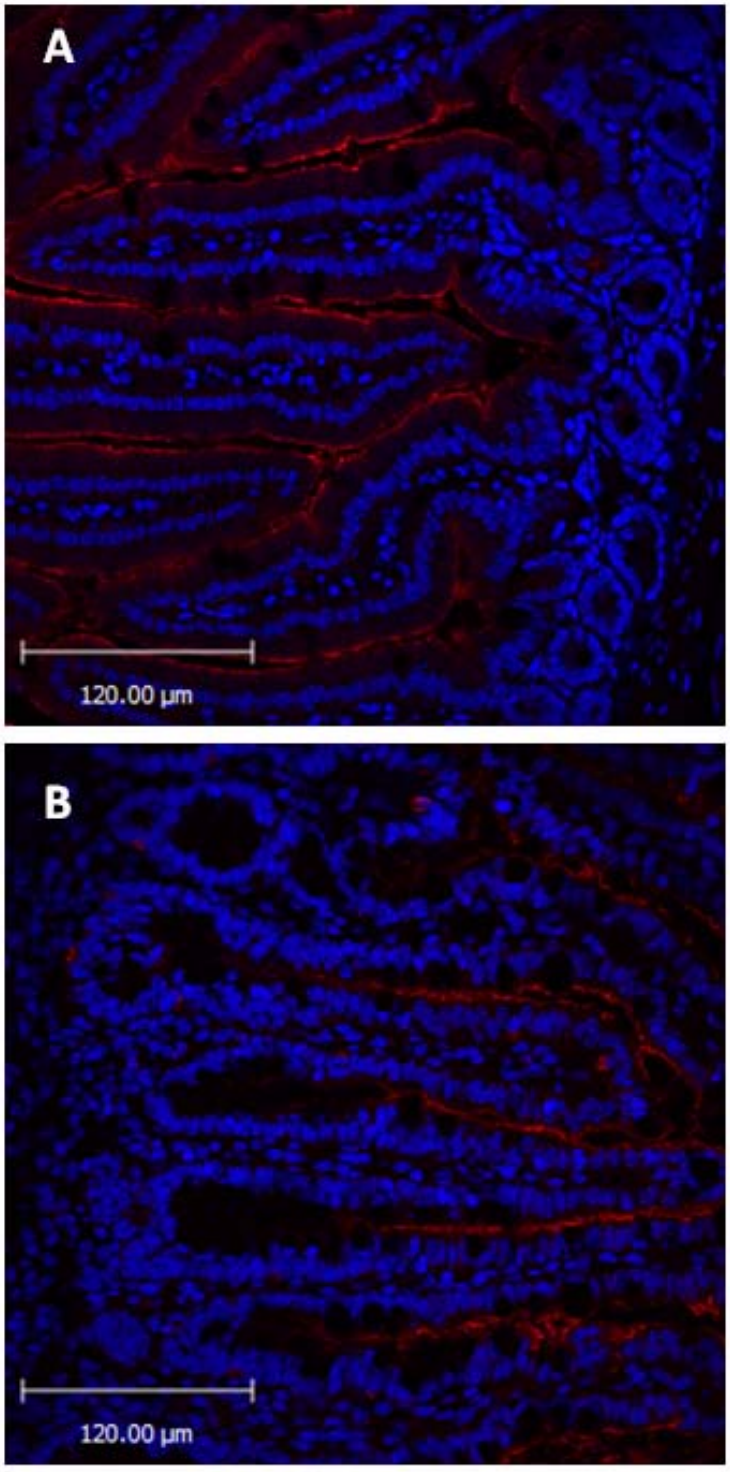

Figure 3.11 Immunofluorescence pictures of mouse (A) and human (B) small intestine paraffin sections. Nucleic acid is stained blue, Alkaline Phosphatase is stained red.

DISCUSSION

An advantage of soft-hydrogel structures for culturing epithelial cells is that they allow for transport away from cells basolaterally, whereas hard or impermeable surfaces do not permit transport through the cell monolayer. Here we took advantage of the biocompatible hydrogel, collagen, to make villous scaffolds capable of supporting human intestinal cell growth in a physically accurate 3D culture. Our modified well insert design protected the scaffolds and insured that they were sealed from short-circuiting. A disadvantage of collagen is that for more rapidly transported drugs, the scaffold becomes the limiting barrier (Figure 3.6). We are investigating alternate hydrogels to determine their appropriateness for rapidly absorbed drug permeability testing.

In the standard protocol, Caco-2 cells need to be cultured for 21 days before the drug permeability test [11]. However, we have found that culturing Caco-2 cells on collagen scaffolds for 21 days not only further shortened the height of the villi, but more importantly, also resulted in the formation of multiple cell layers due to cell penetration and degradation of the collagen, which in our opinion is crucial to avoid in in vitro drug permeability tests [20]. Having multiple cell layers on 2D or 3D collagen scaffolds makes it difficult to compare results to drug permeability tests performed on conventional well inserts in which the test is conducted on a cell monolayer. Hence, in this study we had to conduct the permeability test with collagen scaffolds after culturing Caco-2 cells for 14 days to avoid multiple cell layers forming. To verify that tight junctions were properly formed after 14 days, we compared the permeability

coefficients of Antenolol on conventional well inserts between 14 days culture and 21 days culture. No statistically significant differences were found between the two (Figure 3.12). The confocal scanning of Caco-2 cells cultured for 14 days on 2D collagen (Figure 3.8G) also suggested that a polarized cell monolayer was formed, which is consistent with the high TEER values and low Antenolol permeability coefficients of 2D collagen cultures.

The 3D synthetic villi TEER values and permeability coefficients reflected mammalian intestinal values more accurately than did those for the 2D surfaces. The low TEER value over the 3D collagen synthetic villi matched that reported for a rat ileum (Figure 3.5) and human intestinal epithelia [10]. Our results with Antenolol suggest that there is a difference between cells growing on 2D and 3D surfaces that cannot be explained by the difference in surface area between the two (Figure 3.10). It has been shown that tight junctions increase in leakiness from the tip of the villous to the crypt in normal juvenile intestines [17]. This property of intestinal villi may help explain the permeability difference we found between 3D-grown and 2D-grown monolayers when considered with the pathway through which Antenolol is absorbed. Slowly absorbing drugs, like Antenolol which rely on the paracellular pathway for uptake, may diffuse further along the villi before being absorbed and hence are mostly taken up by cells near the crypts rather than on the villous tips [4]. That this absorption is faster than it would be in 2D culture is supported by confocal data that indicates Caco-2 cells are less differentiated along the lower section of the 3D scaffolds than at the tips (Figure 3.8C–F) as well as cell counts that indicated there was a slightly

higher density of cells near the top of the villi than at the bottom (Figure 3.9). To further prove this point, we investigated in vivo epithelial differentiation of mouse and human small intestines (Figure 3.11). Uneven Alkaline Phosphatase expressions along the crypt-villus axis were only found in human small intestine, which suggested that Caco-2 cells differentiated in an identical way along the crypt-villus axis when comparing to the human while the mouse in vivo model failed to mimic certain human epithelial differentiation characteristics at this point.

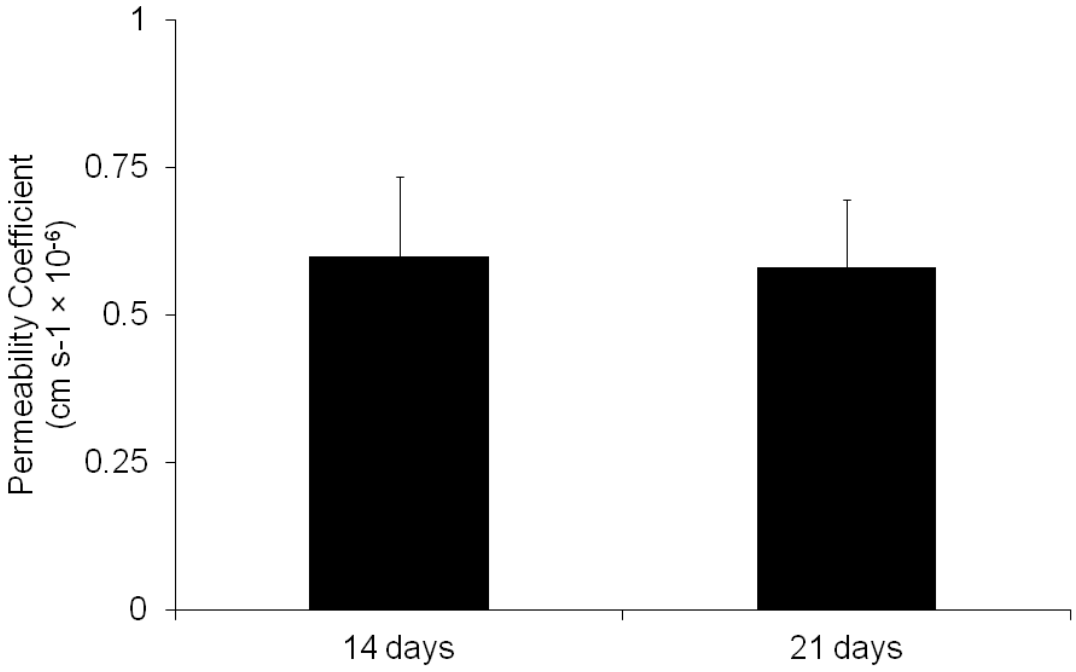

Figure 3.12 Permeability coefficient of Antenolol on Corning 0.4 μm polycarbonate cell culture insert with Caco-2 monolayer cultured 14 days (the same data used in Fig.2b) and Caco-2 monolayer cultured 21 days (the same data used in Fig. SI-3b). No statistically significant differences were found between the two.

While it is clear that cell morphology in the 3D collagen system cannot capture all of the differences between in vitro systems and actual small intestinal epithelium, this study demonstrates the importance of the 3D microenvironment on cell behavior as unique cell differentiation was observed only in the 3D model. We believe that our 3D culturing method using physically mimetic villous scaffolds is more physiologically relevant and therefore more accurate for determining drug permeability coefficients than conventional methods. To further explore the 3D in vitro model, alternative scaffold materials need to be investigated to overcome the transport barrier problem for rapid absorption, which will allow drugs with a wider range of absorption rates to be tested in this 3D in vitro model. This culturing system could also be used to investigate cell differentiation using established stem cell culturing techniques [18] and to begin to understand more completely the role between the physical environment and cellular interactions between human epithelia and microorganisms living in the GI tract.

ACKNOWLEDGEMENTS

This work received support from the National Institutes of Health (DP2 New Innovator Award to JCM), The Hartwell Foundation (Hartwell Investigator Award to JCM), and National Science Foundation (CAREER Award to DL). This work was also supported by the Microscopy and Imaging Facility (MIF) and the Cornell Nanoscale Science and Technology Facility (CNF) at Cornell University. The authors thank Glenn Swan for fabricating the insert kit.

REFERENCES

1. Artursson P (1990) Epithelial transport of drugs in cell culture. I: A model for studying the passive diffusion of drugs over intestinal absorbtive (Caco-2) cells. Journal of Pharmaceutical Sciences 79:476-482

2. Artursson P, Borchardt RT (1997) Intestinal Drug Absorption and Metabolism in Cell Cultures: Caco-2 and Beyond. Pharmaceutical Research 14:1655-1658

3. Artursson P, Karlsson J (1991) Correlation between oral drug absorption in humans and apparent drug permeability coefficients in human intestinal epithelial (Caco-2) cells. Biochemical and Biophysical Research Communications 175:880-885

4. Artursson P, Palm K, Luthman K (2001) Caco-2 monolayers in experimental and theoretical predictions of drug transport. Advanced Drug Delivery Reviews 46:27-43

5. Artursson P, Ungell A-L, Löfroth J-E (1993) Selective Paracellular Permeability in Two Models of Intestinal Absorption: Cultured Monolayers of Human Intestinal Epithelial Cells and Rat Intestinal Segments. Pharmaceutical Research 10:1123-1129

6. Chong S, Dando SA, Soucek KM, Morrison RA (1996) In Vitro Permeability Through Caco-2 Cells is not Quantitatively Predictive of in Vivo Absorption for Peptide-Like Drugs Absorbed via the Dipeptide Transporter System. Pharmaceutical Research 13:120-123

7. Duizer E, Penninks AH, Stenhuis WH, Groten JP (1997) Comparison of permeability characteristics of the human colonic Caco-2 and rat small intestinal IEC-18 cell lines. Journal of Controlled Release 49:39-49

8. Gan L-SL, Thakker DR (1997) Applications of the Caco-2 model in the design and development of orally active drugs: elucidation of biochemical and physical barriers posed by the intestinal epithelium. Advanced Drug Delivery Reviews 23:77-98

9. Hidalgo IJ, Raub TJ, Borchardt RT (1989) Characterization of the human colon carcinoma cell line (Caco-2) as a model system for intestinal epithelial permeability. Gastroenterology 96:736-749

10. Hilgendorf C, Spahn-Langguth H, Regårdh CG, Lipka E, Amidon GL, Langguth P (2000) Caco-2 versus caco-2/HT29-MTX co-cultured cell lines: Permeabilities via diffusion, inside- and outside-directed carrier-mediated transport. Journal of Pharmaceutical Sciences 89:63-75

11. Hubatsch I, Ragnarsson EGE, Artursson P (2007) Determination of drug permeability and prediction of drug absorption in Caco-2 monolayers. Nat. Protocols 2:2111-2119

12. Lennernas H, Ahrenstedt O, Ungell AL (1994) Intestinal drug absorption during induced net water absorption in man; a mechanistic study using antipyrine, atenolol and enalaprilat. British journal of clinical pharmacology 37:589-596

13. Lennernäs H, Palm K, Fagerholm U, Artursson P (1996) Comparison between active and passive drug transport in human intestinal epithelial (caco-2) cells in vitro and human jejunum in vivo. International Journal of Pharmaceutics 127:103-107

14. Linnankoski J, Mäkelä J, Palmgren J, Mauriala T, Vedin C, Ungell A-L, Lazorova L, Artursson P, Urtti A, Yliperttula M (2010) Paracellular porosity and pore

size of the human intestinal epithelium in tissue and cell culture models. Journal of Pharmaceutical Sciences 99:2166-2175

15. Mahler GJ, Esch MB, Glahn RP, Shuler ML (2009) Characterization of a gastrointestinal tract microscale cell culture analog used to predict drug toxicity. Biotechnology and Bioengineering 104:193-205

16. Pinto M, Robine-Leon, S., Appay, Md, Kedinger, M., Triadou, N., Dussaulx, I'.. Lacroix, B.,, Simon-Assmann PH, K., Fogh, J., and Zweibaum, A (1983) Enterocyte-like differentiation and polarization of the human colon carcinoma cell line Caco-2 in culture biology of the cell 47

17. Schulzke J-D, Bentzel CJ, Schulzke I, Riecken E-O, Fromm M (1998) Epithelial Tight Junction Structure in the Jejunum of Children with Acute and Treated Celiac Sprue. Pediatric Research 43:435-441

18. Spence JR, Mayhew CN, Rankin SA, Kuhar MF, Vallance JE, Tolle K, Hoskins EE, Kalinichenko VV, Wells SI, Zorn AM, Shroyer NF, Wells JM (2011) Directed differentiation of human pluripotent stem cells into intestinal tissue in vitro. Nature 470:105-109

19. Sun D, Lennernas H, Welage LS, Barnett JL, Landowski CP, Foster D, Fleisher D, Lee K-D, Amidon GL (2002) Comparison of Human Duodenum and Caco-2 Gene Expression Profiles for 12,000 Gene Sequences Tags and Correlation with Permeability of 26 Drugs. Pharmaceutical Research 19:1400-1416

20. Sung JH, Yu J, Luo D, Shuler ML, March JC (2011) Microscale 3-D hydrogel scaffold for biomimetic gastrointestinal (GI) tract model. Lab on a Chip 11:389-392

21. Tavelin S, Taipalensuu J, Söderberg L, Morrison R, Chong S, Artursson P (2003) Prediction of the Oral Absorption of Low-Permeability Drugs Using Small Intestine-Like 2/4/A1 Cell Monolayers. Pharmaceutical Research 20:397-405

22. Tortora GJ, Grabowski SR (1993) Principles of anatomy and physiology. HarperCollinsCollege, New York

23. Wang L, Murthy SK, Barabino GA, Carrier RL (2010) Synergic effects of crypt-like topography and ECM proteins on intestinal cell behavior in collagen based membranes. Biomaterials 31:7586-7598

CHAPTER FOUR:

POROUS POLY (LACTIC-CO-GLYCOLIC ACID) FOR 3D IN VITRO MODEL OF HUMAN UPPER GASTROINTESTINAL TRACT

Yu J [a], Costello CM [a], Fetcho RN [b],Schaffer CB [b], March JC [*a] (2012) Porous poly (lactic-co-glycolic acid) for 3d in vitro model of human upper gastrointestinal tract.

[a] Biological and Environmental Engineering, Cornell University, USA.
[b] Biomedical Engineering, Cornell University, USA

ABSTRACT

We investigated the potential of using poly (lactic-co-glycolic acid) (PLGA) as a biocompatible material for a 3D in vitro model of human upper gastrointestinal tract. PLGA villous scaffolds were obtained by utilizing a replica molding method. Caco-2 and HT-29 MTX cells were co-cultured on PLGA villous scaffolds to test biocompatibility. To make PLGA villous scaffolds permeable, porogen leaching and laser ablation methods were investigated, which suggested that porous PLGA villous scaffold could be achieved by combining two methods together. Overall, this study showed that PLGA is a good candidate material for 3D in vitro model of human upper gastrointestinal tract.

INTRODUCTION

In vitro models of human gastrointestinal tract have played a critical role for in vitro drug permeability determination [2]. Recently, new stem cell culture techniques have enabled the differentiation of human pluripotent stem cells into functional human small intestine epithelia in vitro [15]. Additionally, 3D biocompatible scaffolds with physiologically relevant dimensions were made by microfabrication techniques to mimic small intestinal villi [16]. These studies not only illustrated a promising way to achieve a better in vitro model for drug permeability determination but also suggested a possibility to make a functional artificial small intestine for treating intestine-related diseases such as short bowel syndrome.

In previous studies, by using collagen villous scaffolds, we have demonstrated that a 3D in vitro model could improve drug permeability testing and present unique cell differentiation characteristics along the crypt-villus axis which were identical to human small intestine epithelia [20]. However, collagen villous scaffolds lack mechanical flexibility and have to preserve its shape in liquid, making it is difficult for transportation and surgical use. Moreover, the permeability of rapidly absorbed drugs in collagen scaffolds was not fast enough to enable testing [20].

In this study, we investigated the potential of using poly (lactic-co-glycolic acid) (PLGA) to fabricate a 3D in vitro human small intestine model. PLGA, as a biocompatible and biodegradable co-polymer material, has been widely used in tissue engineering and approved by the Food and Drug Administration for drug delivery [4, 5, 11]. There are several advantages to use PLGA for making 3D small intestine scaffold. First, PLGA has good mechanical properties [7]. It is not difficult to use it for fabricating high aspect ratio 3D structures at the micrometer scale. Second, various methods have been reported to fabricate a porous PLGA scaffolds including porogen leaching [9], gas foaming [10], emulsion freeze drying [18], phase separation [12] and 3D printing [8]. Third, PLGA has been used as surgical suture material for many years and numerous in vivo studies have suggested that PLGA has excellent biocompatibility and predictable biodegradability [5, 7, 14, 17, 19]. For surgical applications, PLGA has lower chance to induce immunogenicity compared to naturally derived polymer such as collagen. Hence, PLGA is an attractive material for making human small intestinal villi intended for implantation or for in vitro models

that will ultimately have immune components. The goal of this study was to fabricate a porous PLGA villous scaffold with controlled pore size that can allow for passage of small molecules and larger proteins but still prevent cellular invasion.

MATERIALS AND METHODS

Fabrication of PLGA villous scaffold

Polymethylmethacrylate (PMMA) villous template was used to fabricate PLGA scaffold. The fabrication of this PMMA template was described in a previous study [20]. To make a PLGA scaffold, Polydimethylsiloxane (PDMS, Dow Corning, Midland, MI) mixture was poured onto PMMA mold and put into vacuum oven forming PDMS villi structure mold first. The PDMS villi structure mold was then treated by 0.1% (w/w) hydroxypropyl methylcellulose (HPMC, Sigma, St. Louis, MO) solution for 30 min under room temperature to increase the surface hydrophilicity [3]. The HMPC solution was then rinsed, and the PDMS mold was quickly put into a Petri dish and covered by 3 % agarose solution, which gelled to form an agarose template. The PDMS mold was gently pilled off the agarose template and the agarose template was air-dried an hour to evaporate water residue inside the template holes. 10% (w/v) PLGA (85:15, Durect Corporation, Birmingham, AL) in chloroform solution was added to agarose template and put into vacuum oven right away to remove any gas inside holes. Then the agarose template with PLGA was left in chemical hood for 3 hours to evaporate all the chloroform solvent. Due to the flexibility of agarose and PLGA, the PLGA villous scaffold can be obtained by gently pilling off the agarose template. The whole fabrication process was illustrated in Figure 4.1.

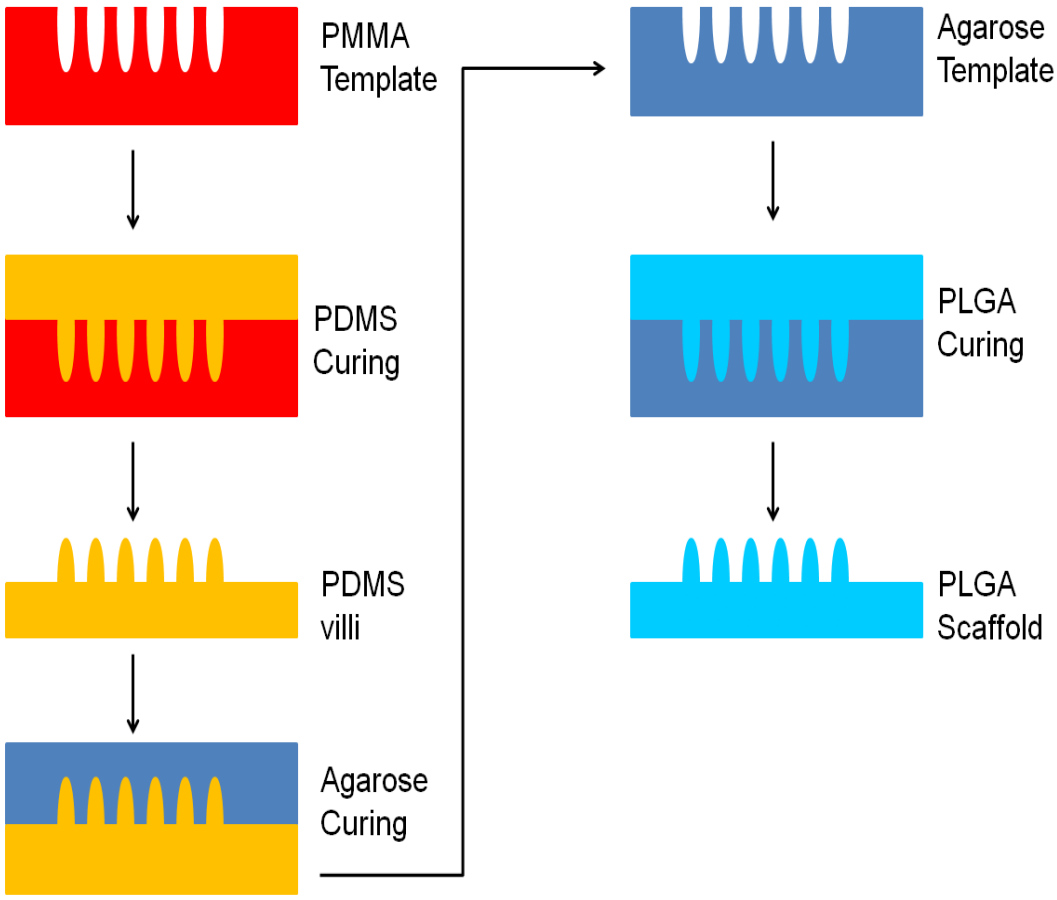

Figure 4.1 Fabrication process of the PLGA villous scaffold

Cell culture

The human colon carcinoma cell line Caco-2 (passage number 16-25, ATCC, Manassas, VA) HT29-MTX (passage number 39-49, a kind gift from Professor Michael L. Shuler, Cornell University) were used in this study. Both cell lines were maintained in Dulbecco's Modified Eagle's Media (Mediatech, Manassas, VA), with 10% FBS (Invitrogen, Carlsbad, CA) and 1X anti-biotic anti-mycotic (Invitrogen). For coculture on PLGA scaffolds, PLGA scaffolds were sterilized in 70% ethanol

overnight and washed with PBS for 3 days. Caco-2 and HT29-MTX cells were seeded on PLGA scaffolds with a 3:1 ratio (Caco-2:HT29-MTX) at 1×10^6 cells/ml seeding density. Media was exchanged 1 day after seeding and every 2 days during the experiment.

Fabrication of PLGA villous scaffold using porogen leaching method

Sucrose fine powder was mixed with ammonium bicarbonate fine powder with 1 to 1 weight ratio. The powder mixture was further fined by hand using mortar and pestle for 30 min. Then the powder mixture was add to 10% (w/v) PLGA (85:15, Durect Corporation) in chloroform and a homogenizer (model μH, Omni International, Kennesaw, GA) was used to mix the powder with PLGA-chloroform solution. Right after the homogenizer mixing, the solution mixture was added to agarose template and put into vacuum oven for removing gas bubbles. Then agarose template with PLGA mixture on top was left in chemical hood for 3 hours and then submerged in 45 °C water overnight to dissolve all the porogens.

Laser ablation on PLGA scaffold

Laser ablation was performed at Professor Chris B. Schaffer's Lab at Cornell University using a Femtosecond laser system including a Ti:Sapphire regenerative amplifier (Legend 1k USP, Coherent Inc, Santa Clara, CA), a Q-switched laser (Evolution 15, Coherent Inc.) and a Ti:Sapphire oscillator (Kapteyn-Murnane Laboratories Inc., Boulder, CO). Real time image was obtained by using a custom-designed two-photon excited fluorescence microscope utilizing a modelocked

Ti:Sapphire laser (Chameleon, Coherent Inc.). PLGA scaffold was stained by 1:1000 diluted TO-PRO-3 (Invitrogen) solution overnight to generate enough fluorescence. A 20X magnification, water-immersion objective (Zeiss, Thornwood, NY) was used with the two-photon excited fluorescence microscope

Dye Test

PLGA villous scaffolds were assembled in custom-made insert kits. Details of the insert kit were described in a previous study [20]. NEON blue food dye solution (McCormick & Co, Hunt Valley, MD) was added to the apical side of the insert kit. A wiper paper was used to detect if any dye was able to pass through PLGA villous scaffolds.

Microscopy

For Scanning electron microscope (SEM), PLGA samples were coated by an Au-Pd sputter coater (Denton DESK II, Denton Vacuum, Moorestown, NJ). Leica Stereoscan 440 Scanning electron microscope (Leica Microsystems, Buffalo Grove, IL) was used to exam the sample. For confocal microscope, cell samples were stained by Alexa Fluor 488 phalloidin (Invitrogen) and TO-PRO-3 for actin and nucleic acid staining, respectively. Leica SP2 confocal microscope (Leica Microsystems, Buffalo Grove, IL) was used to scan the sample. 3D rendering images and section pictures were assembled with Volocity 5.0 software (Perkin Elmer, Waltham, MA).

RESULTS

PLGA villous scaffold can be made by replica molding method due to its good mechanical properties. Agarose gel was chosen as the final template based on two reasons. First, the chloroform solvent of PLGA could easily destroy the PMMA template. Second, the agarose gel is soft and flexible, which provided a good protection of the villous shape when PLGA scaffold was peeled off the agarose template. SEM pictures showed that the final PLGA scaffold processed villi array as designed that each villus has full high aspect ratio shape and smooth curvature (Figure 4.2).

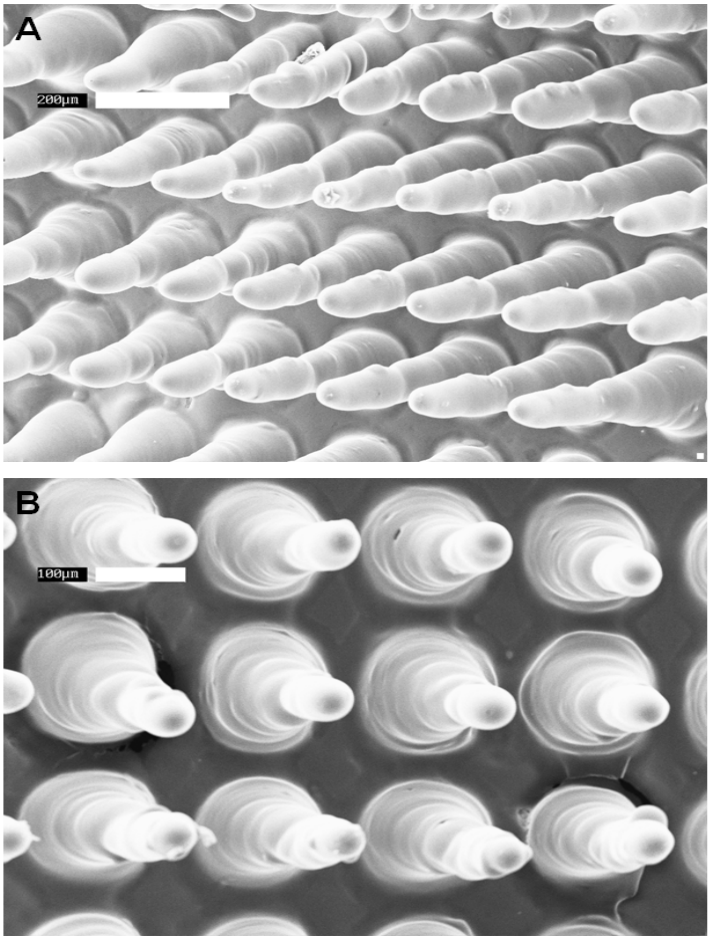

Figure 4.2 SEM pictures of the PLGA villous scaffold with (A) low magnification and (B) high magnification.

Caco-2 and HT-29 MTX were co-cultured on the PLGA villous scaffold to mimic the small intestinal enterocytes and goblet cells respectively. PLGA itself could support Caco-2 and HT-29 MTX proliferation along the villus without any collagen or Matrigel coating (Figure 4.3), which proved its excellent biocompatibility characteristic. However, even with collagen coating, cells on PLGA scaffolds failed to sustain proliferation and differentiation over a certain culture time, which suggested that there were limitations to either nutrient transport to or waste transport away from the cells as they grew. We hypothesized that basolateral feeding may allow longer culture times.

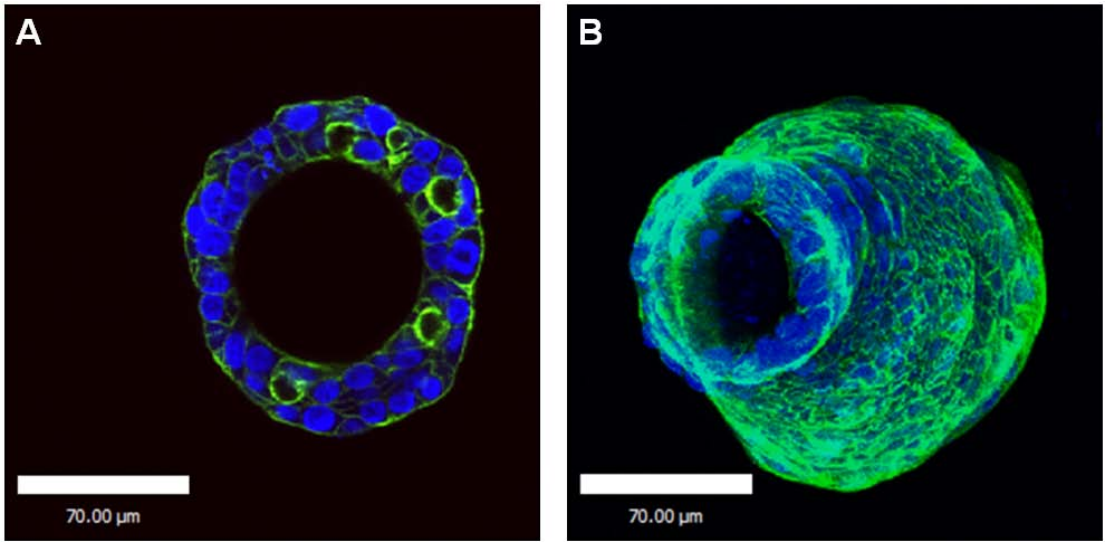

Figure 4.3 Confocal pictures of Caco-2 and HT-29 MTX cocultured on the PLGA villous scaffold. (A) X-Y section picture (B) 3D rendering picture of a single villus. Cells are stained green (actin) and blue (nucleic acid).

A porogen leaching method was utilized to make porous PLGA villous scaffold. By controlling porogen particle size, less than 10 μm holes were obtained on PLGA scaffold surface (Figure 4.4). It is need to note that the PLGA scaffold lost some mechanical strength and became fragile after being made using porogen leaching method. But overall it is still strong enough that PLGA villi do not need to be preserved in liquid phase.

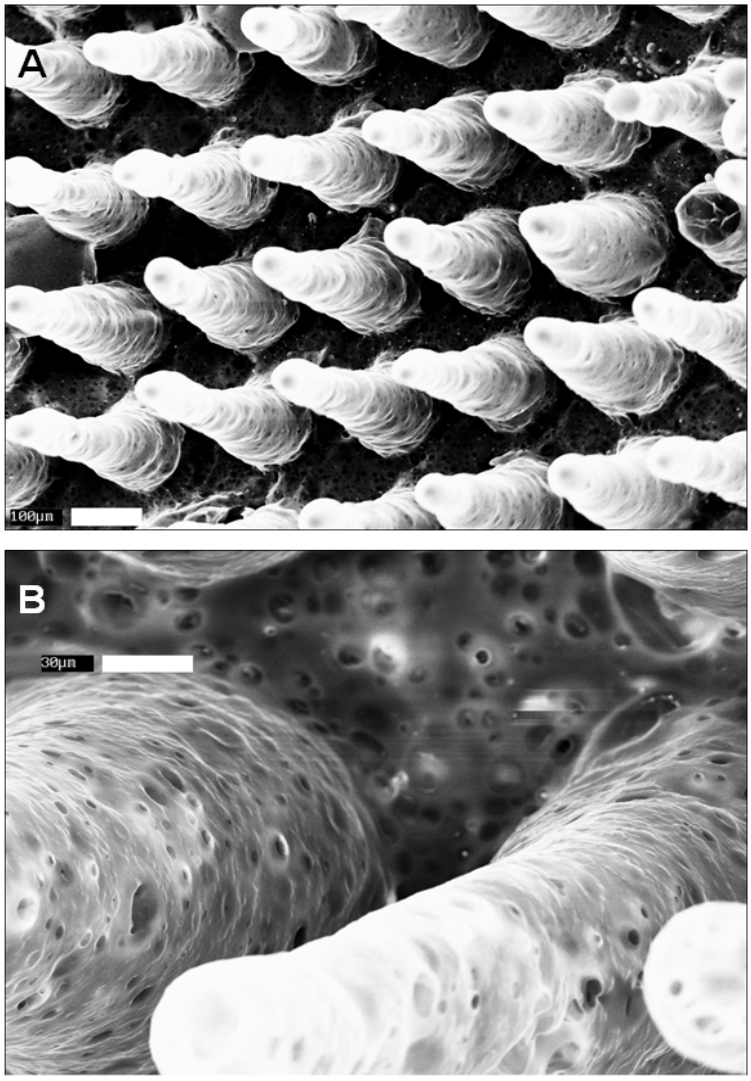

Figure 4.4 SEM pictures of the PLGA villous scaffold made by porogen leaching method with (A) low magnification and (B) high magnification.

A femtosecond laser ablation method was also tested on PLGA scaffolds since it has been used to successfully fabricate high aspect ratio microcapillaries on PDMS device [6]. The primary result suggested that the diameter of the hole on PLGA surface can be controlled within 10μm, which is small enough to block epithelial cells. Hence, it is possible to use femtosecond laser ablation to create micro sized channels on PLGA villous scaffold, which makes it similar as the commercially available membranes made by track etching technique [1]. Dye test results also suggested that PLGA villous scaffold treated by the laser ablation became permeable to dye solution, which proved the functionality of holes (Figure 4.6).

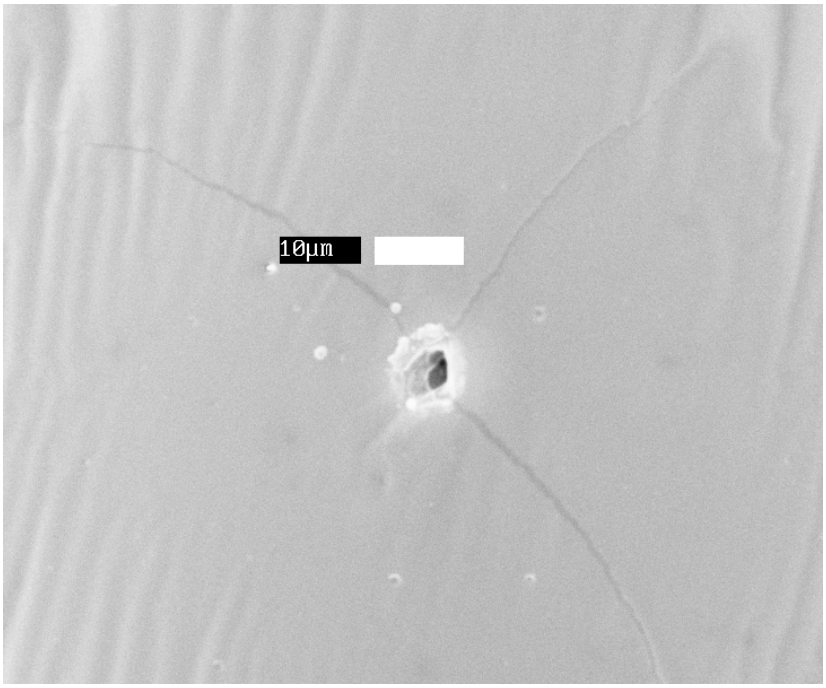

Figure 4.5 SEM picture of the PLGA scaffold with a single hole drilled by laser

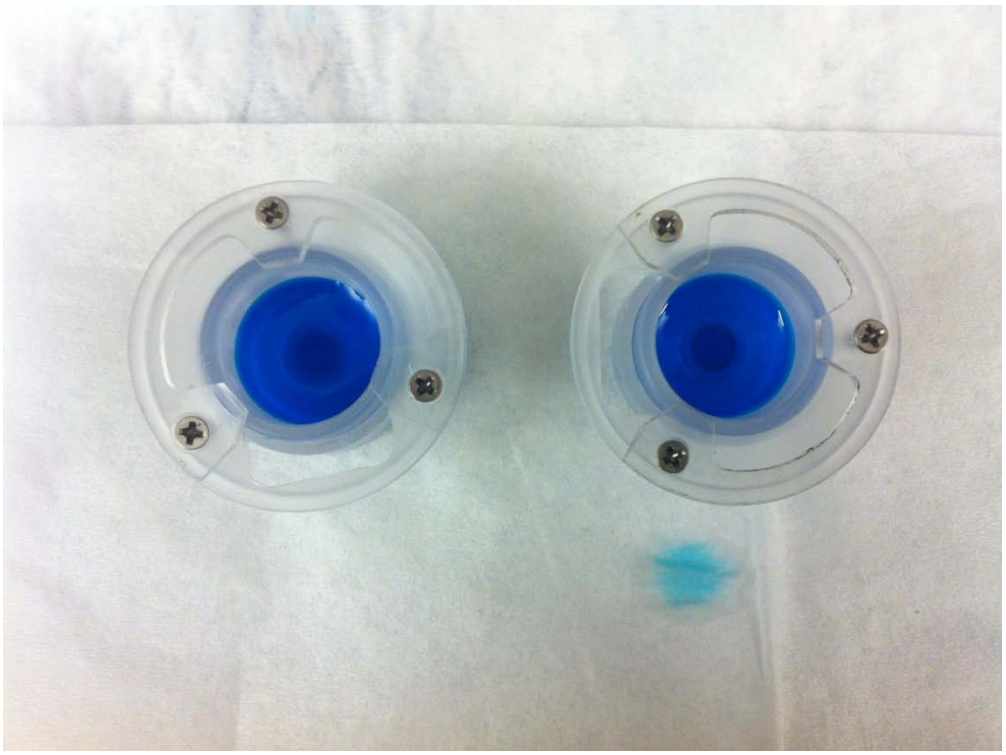

Figure 4.6 Dye test results of a PLGA villous scaffold without laser drilling (left) and a PLGA villous scaffold with laser drilling (right)

DISCUSSION

The advantage of PLGA is that, due to its good mechanical properties, a PLGA villous scaffold can be made just using replica molding method, which is much easier when compared to the method used for making collagen villous scaffolds [16]. However, cell culture on PLGA needs to be improved to show that fully differentiated epithelial cells can be achieved on PLGA villous scaffold. Hence, having a porous villous scaffold is crucial that it not only provides the ability to feed epithelial cells from basolateral side which is physiological relevant comparing to in vivo epithelial cell feeding but also makes PLGA scaffold useful for in vitro drug permeability

determination [13]. Porogen leaching and femtosecond laser ablation results suggested two different ways to make PLGA porous. The challenging part is to make porous PLGA scaffold when still preserving the villous structure. Combining two methods together in the future research that using the laser ablation to interconnect holes created by porogens could possibly obtains an ideal porous PLGA villous scaffold. Overall, this primary study suggested that PLGA is a good candidate material for making 3D villous scaffold.

ACKNOWLEDGEMENTS

This work received support from the National Institutes of Health (DP2 New Innovator Award to JCM). This work was also supported by Microscopy and Imaging Facility (MIF) at Cornell University. The authors thank Professor Michael L. Shuler and Professor Chris B. Schaffer at Cornell University for providing experiment materials.

REFERENCES

1. Apel P (2001) Track etching technique in membrane technology. Radiation Measurements 34:559-566
2. Artursson P, Palm K, Luthman K (2001) Caco-2 monolayers in experimental and theoretical predictions of drug transport. Advanced Drug Delivery Reviews 46:27-43
3. Gitlin L, Schulze P, Belder D (2009) Rapid replication of master structures by double casting with PDMS. Lab on a Chip 9:3000-3002

4. Ignatius AA, Claes LE (1996) In vitro biocompatibility of bioresorbable polymers: poly(L, DL-lactide) and poly(L-lactide-co-glycolide). Biomaterials 17:831-839

5. Jain RA (2000) The manufacturing techniques of various drug loaded biodegradable poly(lactide-co-glycolide) (PLGA) devices. Biomaterials 21:2475-2490

6. Kim TN, Campbell K, Groisman A, Kleinfeld D, Schaffer CB (2005) Femtosecond laser-drilled capillary integrated into a microfluidic device. Applied Physics Letters 86:201106-201106-201103

7. Kitchell JP, Wise DL (1985) [32] Poly(lactic/glycolic acid) biodegradable drug—polymer matrix systems. In: Kenneth J. Widder RG (ed) Methods in Enzymology. Academic Press, p 436-448

8. Lee M, Dunn JCY, Wu BM (2005) Scaffold fabrication by indirect three-dimensional printing. Biomaterials 26:4281-4289

9. Mikos AG, Sarakinos G, Leite SM, Vacant JP, Langer R (1993) Laminated three-dimensional biodegradable foams for use in tissue engineering. Biomaterials 14:323-330

10. Mooney DJ, Baldwin DF, Suh NP, Vacanti JP, Langer R (1996) Novel approach to fabricate porous sponges of poly(d,l-lactic-co-glycolic acid) without the use of organic solvents. Biomaterials 17:1417-1422

11. Murphy WL, Peters MC, Kohn DH, Mooney DJ (2000) Sustained release of vascular endothelial growth factor from mineralized poly(lactide-co-glycolide) scaffolds for tissue engineering. Biomaterials 21:2521-2527

12. Nam YS, Park TG (1999) Biodegradable polymeric microcellular foams by modified thermally induced phase separation method. Biomaterials 20:1783-1790

13. Perdikis DA, Basson MD (1997) Basal nutrition promotes human intestinal epithelial (Caco-2) proliferation, brush border enzyme activity, and motility. Critical Care Medicine 25:159-165

14. Ramchandani M, Robinson D (1998) In vitro and in vivo release of ciprofloxacin from PLGA 50:50 implants. Journal of Controlled Release 54:167-175

15. Spence JR, Mayhew CN, Rankin SA, Kuhar MF, Vallance JE, Tolle K, Hoskins EE, Kalinichenko VV, Wells SI, Zorn AM, Shroyer NF, Wells JM (2011) Directed differentiation of human pluripotent stem cells into intestinal tissue in vitro. Nature 470:105-109

16. Sung JH, Yu J, Luo D, Shuler ML, March JC (2011) Microscale 3-D hydrogel scaffold for biomimetic gastrointestinal (GI) tract model. Lab on a Chip 11:389-392

17. Uematsu K, Hattori K, Ishimoto Y, Yamauchi J, Habata T, Takakura Y, Ohgushi H, Fukuchi T, Sato M (2005) Cartilage regeneration using mesenchymal stem cells and a three-dimensional poly-lactic-glycolic acid (PLGA) scaffold. Biomaterials 26:4273-4279

18. Whang K, Thomas CH, Healy KE, Nuber G (1995) A novel method to fabricate bioabsorbable scaffolds. Polymer 36:837-842

19. Yoon E, Dhar S, Chun DE, Gharibjanian NA, Evans GR (2007) In vivo osteogenic potential of human adipose-derived stem cells/poly lactide-co-glycolic acid constructs for bone regeneration in a rat critical-sized calvarial defect model. Tissue engineering 13:619-627

20. Yu J, Peng S, Luo D, March JC (2012) In vitro 3D human small intestinal villous model for drug permeability determination. Biotechnology and Bioengineering 109:2173-2178

CHAPTER FIVE:

CONCLUSIONS

The challenges of improving current human small intestine in vitro models mainly come from two aspects. The first challenge is to find a suitable material for fabricating 3D scaffolds. The material has to be capable of supporting epithelial cells forming a differentiated monolayer over long term culture, and the material has to be permeable enough so that it does not present a significant barrier for nutrient and drug transport. The fast development of biomaterials, especially various hydrogel techniques over last two decades, has already had profound impact on tissue engineering [2]. Apart from materials we described in previous chapters, we also tested other hydrogels. For example, we started with a simple idea involving the use of a Matrigel-coated agarose hydrogel for epithelial cell culture. We found that since Matrigel did not immobilize effectively onto the agarose surface, it could not actually promote epithelial cell attachment and proliferation. Subsequently, we used a chemical modification method to covalently bind RGD (Arg-Gly-Asp) peptides to PEGDA (Poly (ethylene glycol) diacrylate) hydrogels [3], and we achieved some success in promoting cell attachment and proliferation. However, we discovered that there was a limit to the maximum concentration of RGD which could be bound to PEGDA hydrogels, making this method inadequate for actually supporting Caco-2 cell proliferation and differentiation into a functional monolayer. Furthermore, we tested the idea of mixing PEGDA with collagen. Unfortunately, it was very difficult to verify that collagen and PEGDA were well mixed during the photopolymerization. Hence, finding a suitable material will always be the main challenge of this project, especially with the consideration that the materials also need to be capable of being made into the 3D villous shape.

The second challenge is to establish new epithelial cell lines with more physiologically relevant characteristics for the in vitro model. The Caco-2 cell line has been used since the very first small intestine in vitro model. The co-culture of Caco-2 and HT29-MTX further improved physiological relevance, although the other two epithelial cell types were still missing. Since both Caco-2 and HT29-MTX were isolated as colon carcinoma cell lines, to some extent, they still possess different characteristics when compared to normal human small intestine epithelial cells [7]. Recently, emerging stem cell culture techniques have suggested the possibility of differentiating human stem cells into the intestinal tissue with all four small intestine epithelial cell types in vitro [6]. Utilizing the advancing stem cell isolation and culture techniques could greatly improve the conventional in vitro model.

Since this 3D small intestine in vitro model was developed as a research tool, it can be applied to following future research directions. The first direction is to continue exploring the potential of using a 3D model for improving drug permeability correlations, especially if a better material can be found to overcome the transportation barrier problem. The second direction is to combine the stem cell techniques with the 3D scaffold in order to fabricate an artificial human small intestine for treating short bowel syndrome. Currently there is no effective way for treating short bowel syndrome. Seeding stem cells on the 3D scaffold and thus forming a functional artificial small intestine in vitro for subsequent implantation may provide a cure for this fatal disease. The third direction is to use this 3D model for investigating the interactions between commensal bacteria and small intestine epithelia. There is a large

population of commensal bacteria located in human intestine [4]. Understanding communication and interactions between commensal bacteria and small intestinal epithelia may help in the study of the causes of intestine-related diseases [1, 5]. Overall, the 3D small intestine in vitro model can be a powerful tool for intestine-related research.

REFERENCES

1. Darfeuille-Michaud A, Boudeau J, Bulois P, Neut C, Glasser A-L, Barnich N, Bringer M-A, Swidsinski A, Beaugerie L, Colombel J-F (2004) High prevalence of adherent-invasive Escherichia coli associated with ileal mucosa in Crohn's disease. Gastroenterology 127:412-421
2. Drury JL, Mooney DJ (2003) Hydrogels for tissue engineering: scaffold design variables and applications. Biomaterials 24:4337-4351
3. Hern DL, Hubbell JA (1998) Incorporation of adhesion peptides into nonadhesive hydrogels useful for tissue resurfacing. Journal of Biomedical Materials Research 39:266-276
4. Kleerebezem M, Vaughan EE (2009) Probiotic and Gut Lactobacilli and Bifidobacteria: Molecular Approaches to Study Diversity and Activity. Annual Review of Microbiology 63:269-290
5. Murray JA (1999) The widening spectrum of celiac disease. The American Journal of Clinical Nutrition 69:354-365
6. Spence JR, Mayhew CN, Rankin SA, Kuhar MF, Vallance JE, Tolle K, Hoskins EE, Kalinichenko VV, Wells SI, Zorn AM, Shroyer NF, Wells JM

(2011) Directed differentiation of human pluripotent stem cells into intestinal tissue in vitro. Nature 470:105-109

7. Sun D, Lennernas H, Welage LS, Barnett JL, Landowski CP, Foster D, Fleisher D, Lee K-D, Amidon GL (2002) Comparison of Human Duodenum and Caco-2 Gene Expression Profiles for 12,000 Gene Sequences Tags and Correlation with Permeability of 26 Drugs. Pharmaceutical Research 19:1400-1416